NASA / CR—1999-208884 PWA 6420–103

TFaNS Tone Fan Noise Design / Prediction System

Volume III: Evaluation of System Codes

David A. Topol
United Technologies Corporation, East Hartford, Connecticut

March 1999

The NASA STI Program Office . . . in Profile

Since its founding, NASA has been dedicated to the advancement of aeronautics and space science. The NASA Scientific and Technical Information (STI) Program Office plays a key part in helping NASA maintain this important role.

The NASA STI Program Office is operated by Langley Research Center, the Lead Center for NASA's scientific and technical information. The NASA STI Program Office provides access to the NASA STI Database, the largest collection of aeronautical and space science STI in the world. The Program Office is also NASA's institutional mechanism for disseminating the results of its research and development activities. These results are published by NASA in the NASA STI Report Series, which includes the following report types:

- TECHNICAL PUBLICATION. Reports of completed research or a major significant phase of research that present the results of NASA programs and include extensive data or theoretical analysis. Includes compilations of significant scientific and technical data and information deemed to be of continuing reference value. NASA's counterpart of peer-reviewed formal professional papers but has less stringent limitations on manuscript length and extent of graphic presentations.

- TECHNICAL MEMORANDUM. Scientific and technical findings that are preliminary or of specialized interest, e.g., quick release reports, working papers, and bibliographies that contain minimal annotation. Does not contain extensive analysis.

- CONTRACTOR REPORT. Scientific and technical findings by NASA-sponsored contractors and grantees.

- CONFERENCE PUBLICATION. Collected papers from scientific and technical conferences, symposia, seminars, or other meetings sponsored or cosponsored by NASA.

- SPECIAL PUBLICATION. Scientific, technical, or historical information from NASA programs, projects, and missions, often concerned with subjects having substantial public interest.

- TECHNICAL TRANSLATION. English-language translations of foreign scientific and technical material pertinent to NASA's mission.

Specialized services that complement the STI Program Office's diverse offerings include creating custom thesauri, building customized data bases, organizing and publishing research results . . . even providing videos.

For more information about the NASA STI Program Office, see the following:

- Access the NASA STI Program Home Page at ***http://www.sti.nasa.gov***

- E-mail your question via the Internet to help@sti.nasa.gov

- Fax your question to the NASA Access Help Desk at (301) 621-0134

- Telephone the NASA Access Help Desk at (301) 621-0390

- Write to:
  NASA Access Help Desk
  NASA Center for AeroSpace Information
  7121 Standard Drive
  Hanover, MD 21076

NASA / CR—1999-208884 PWA 6420–103

TFaNS Tone Fan Noise Design / Prediction System

Volume III: Evaluation of System Codes

David A. Topol
United Technologies Corporation, East Hartford, Connecticut

Prepared under Contract NAS3–26618

National Aeronautics and
Space Administration

Glenn Research Center

March 1999

Available from

NASA Center for Aerospace Information
7121 Standard Drive
Hanover, MD 21076
Price Code: A04

National Technical Information Service
5285 Port Royal Road
Springfield, VA 22100
Price Code: A04

FOREWORD

This report was prepared under NASA Contract NAS3−26618, Tasks 4 and 4A for the NASA Lewis Research Center. The NASA Task Manager was Dennis Huff. Pratt & Whitney's Task Manager was D. A. Topol. The author gratefully acknowledges D. B. Hanson, H. D. Meyer, W. Eversman, D. C. Mathews, and E. Envia for their help and useful suggestions which helped make the development of this system possible.

The author also wishes to thank Micah L. Abelson, who, while as a Cooperative Education Student at Pratt & Whitney, worked with the author to develop criteria for determining the number of rotor and stator integration stations in the SOURCE3D code.

TABLE OF CONTENTS

Section	Title	Page
SUMMARY		**1**
1.	**BACKGROUND**	**2**
2.	**COUPLING AND NOISE PREDICTION SCHEME**	**4**
3.	**GENERAL ORGANIZATION OF TFaNS**	**6**
4.	**SOUND POWER LEVEL EVALUATION OF TFANS**	**8**
4.1	Evaluation with Full Scale Engine Data	8
4.2	Evaluation with ADP 22” RIG FAN1 Data	12
4.3	Preliminary Conclusions from the TFaNS Power Level Evaluation	19
4.4	Investigating the Effects of the 2D Aerodynamic/3D Acoustic Interface in SOURCE3D	21
5.	**FAR−FIELD SOUND PRESSURE LEVEL TFaNS EVALUATION USING ADP 22” RIG DATA**	**25**
6.	**CONCLUSIONS**	**30**
7.	**RECOMMENDATIONS**	**32**
8.	**REFERENCES**	**33**
Appendix I: Development and Evaluation of SOURCE3D Chordwise Integration Station Criteria		**35**

SUMMARY

TFaNS is the Tone Fan Noise Design/Prediction System developed by Pratt & Whitney under contract to NASA Lewis. The purpose of this system is to predict tone noise emanating from a fan stage including the effects of reflection and transmission by the rotor and stator and by the duct inlet and nozzle. These effects have been added to an existing annular duct/isolated stator noise prediction capability.

The underlying concept for the system was presented in Reference 1 with application to cascades in 2−dimensional channels. TFaNS extends this to annular geometry with duct terminations and radiation to the far−field via the following scheme: "Acoustic elements" (e.g. the inlet, the rotor, the stator, and the nozzle) are first analyzed in isolation to determine their modal reflection and transmission coefficients (including frequency scattering in the case of the rotor). Then the elements are coupled as a linear system via the duct eigenmodes at "interface planes" separating the elements. The linear system is solved to find a "state vector" of mode amplitudes at the interface planes. The "state vector" then is used to compute upstream and downstream modal sound powers and the sound pressure directivities in the outside field.

TFaNS consists of:

- The codes that compute the acoustic properties (reflection and transmission coefficients) of the various elements and writes them to files,
- CUP3D: Fan Noise Coupling Code that reads these files, solves the coupling equations, and outputs the desired noise predictions,
- AWAKEN: CFD/Measured Wake Postprocessor which reformats CFD wake predictions and/or measured wake data so they can be used by the system to predict noise.

This document evaluates TFaNS versus full−scale and ADP 22" rig data using the semi−empirical wake modelling presently in the system. No CFD or measured wakes are used in this evaluation and AWAKEN is not included in this evaluation.

Technical documentation of the TFaNS codes is given in References 2 through 8. The TFaNS User's Manual may be found in Reference 9.

1. BACKGROUND

Several sources contribute to fan tone noise in turbofan engines. Of these, fan wake/FEGV interactions have long been recognized to be one of the important tone noise sources. Under certain circumstances, the reflection and transmission of this noise source through the rotor have been found to be significant. In 1987, Topol, Holhubner and Mathews (Reference 10) observed that a FEGV generated forward travelling spinning mode at blade passing frequency (BPF) cuts on earlier in the swirl region between the fan and the FEGV than just upstream of the fan or just downstream of the FEGV. They further observed that when this mode reaches the fan, it reflects off the fan at higher BPF harmonics which travel back through the FEGV's to the far−field and becomes important in the far−field. Full scale engine and fan rig data were used to support these observations. Also in the 1987 paper, a simple model was presented which qualitatively reproduced this behavior.

Figure 1, from Reference 10, shows measured aft sound power level full scale engine data which supports this "wave reflection" behavior. In this figure, when forward propagating BPF noise due to fan wake/FEGV interaction noise cuts on in the swirl region between the fan and the FEGV's, aft 2BPF and 3BPF noise rises rapidly.

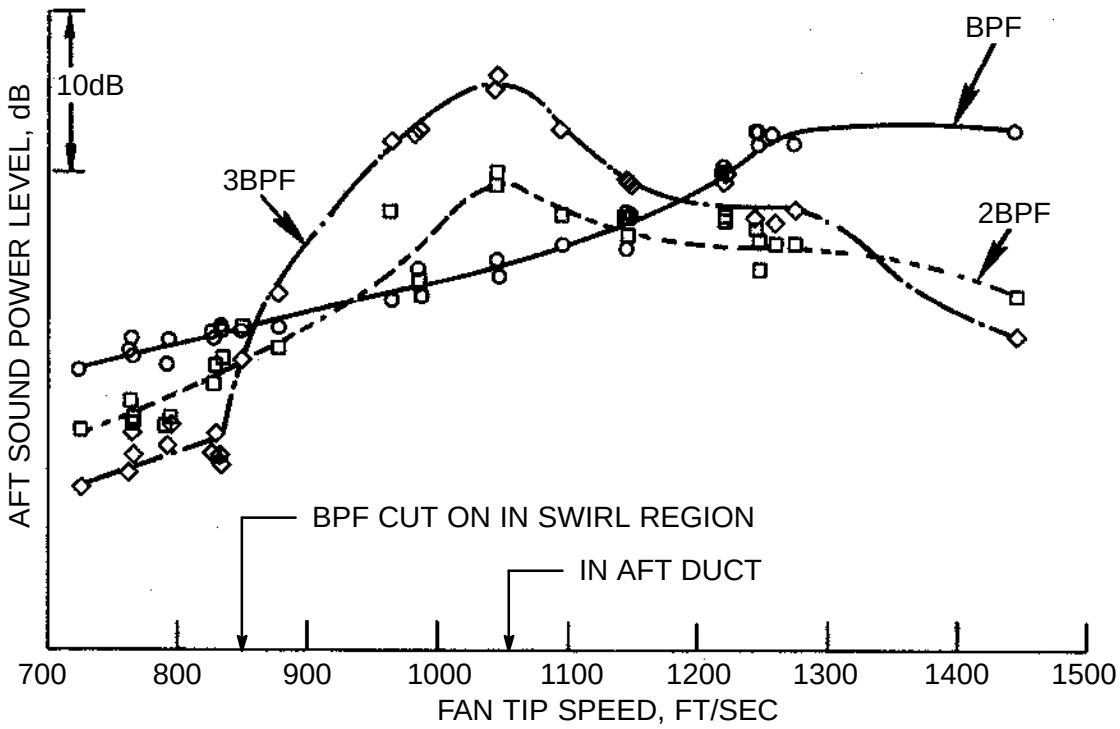

Figure 1: Measured Aft Radiated Noise for Full Scale Engine Data (from References 1 and 10)

Furthermore, as the vane/blade ratio was increased, the sudden rise in aft 3BPF was postponed to a higher speed (see Figure 2). This is consistent with the higher speed at which BPF cut on in the swirl region as is seen in Figure 2.

Work has been done since then to more effectively model this noise behavior. Hanson (References 1, 11, and 12) modelled this problem in two dimensions using the Smith code (Reference 13) as a starting point. In these papers he showed that it was the effect of flow turning that most affected this problem. He labeled the behavior discussed above "mode trapping". i.e. modes which are cut on within the swirl

region between the fan and FEGV's, but cut off outside the swirl region are "trapped" between the fan and the FEGV. However, when they are scattered into other BPF harmonics, they can contribute to the far−field.

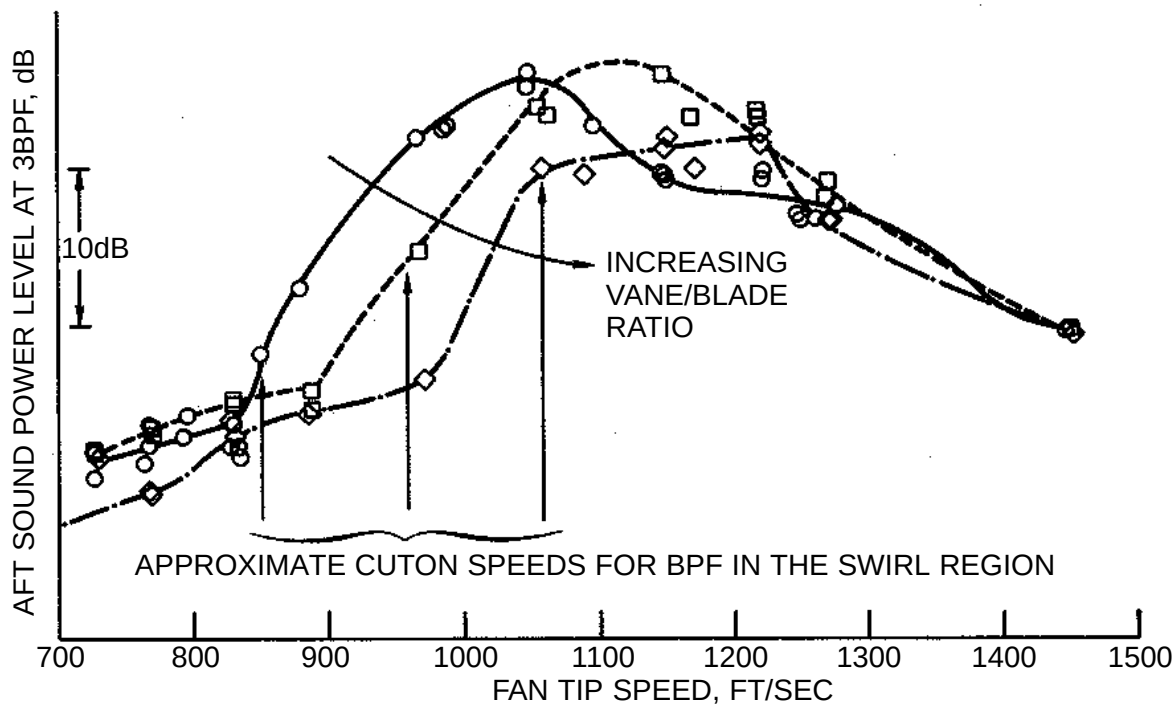

Figure 2: Measured Aft Radiated Noise for 3 Vane/Blade Ratios (from Reference 10)

In Reference 1, Hanson outlined a method for handling this problem in three dimensions. He suggested that treating the engine as a series of "acoustic elements" (e.g. inlet, rotor, stator, exit) as in Figure 3 (see the next section) would permit the use of a series of computer codes which would model these elements separately. Code developers could then use non−reflecting boundary conditions to represent each acoustic element's computational boundaries (as code developers often assume in existing analyses). A fan noise coupling code could then be developed to couple the system.

This report presents the evaluation of just such a system based on the formulation in Reference 1 which is referred to as the TFaNS Tone Fan Noise design/prediction System. The system consists of modified versions of a rotor/stator interaction code, inlet radiation code, and aft radiation code. The system's technical documentation, as evaluated in this document, is found in References 2 through 7.

The next section discusses, in general, the coupling and noise prediction scheme. The general organization of the system is then presented. This is followed by the system evaluation with full scale engine and ADP 22" fan rig data on a sound power level basis. ADP rig far−field directivities are also presented. From these results, conclusions and recommendations for future work are given.

This report also includes Appendix I which explains the development of the rotor chordwise integration station criterion being used by the SOURCE3D Rotor Wake/Stator Interaction code. The stator chordwise integration station criterion and the rotor and stator radial integration station criteria are explained in Reference 14.

2. COUPLING AND NOISE PREDICTION SCHEME

The TFaNS coupling and noise prediction scheme is explained conceptually with reference to Figure 3.

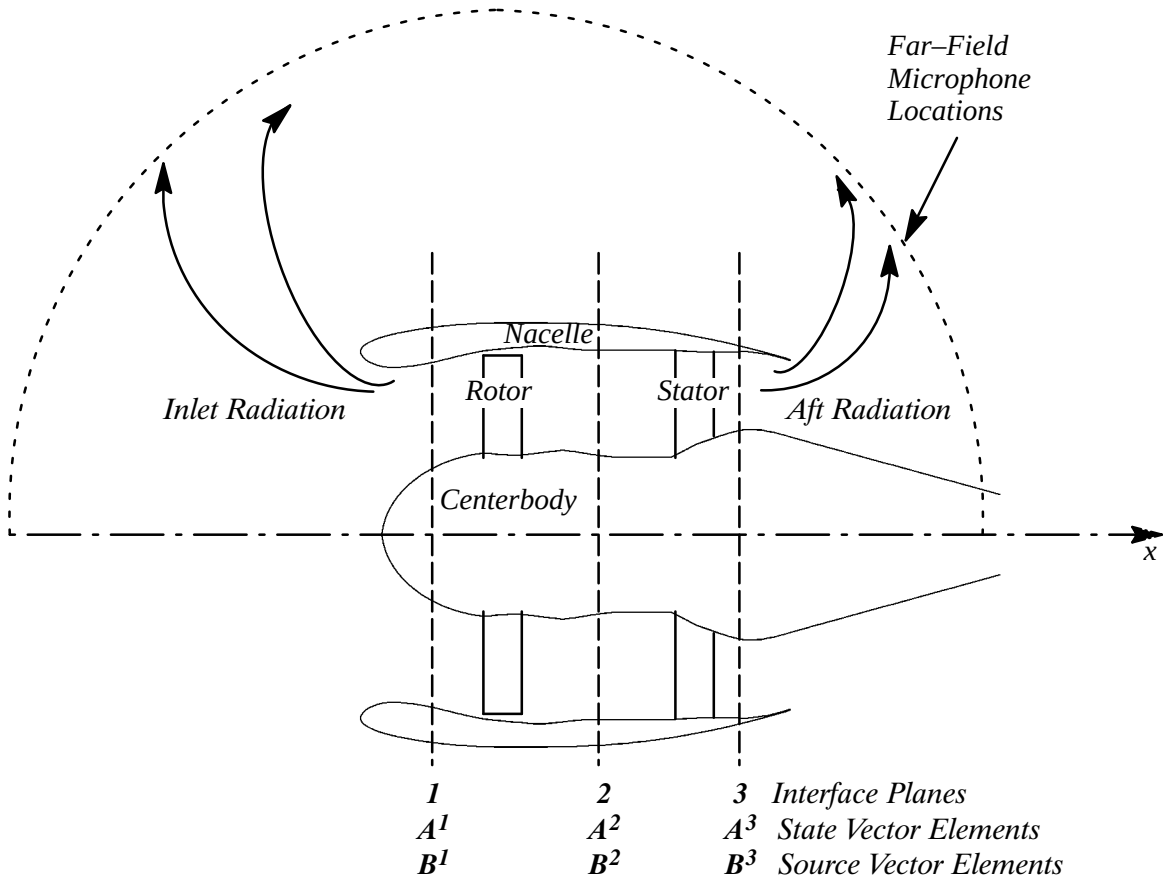

Figure 3: TFaNS Coupling and Noise Prediction Scheme

The fan stage is divided by three interface planes into four acoustic elements (inlet, rotor, stator, and nozzle). State vector, $\boldsymbol{A}$, is in three sections, $\boldsymbol{A^1}$, $\boldsymbol{A^2}$, and $\boldsymbol{A^3}$, whose structure is in terms of modal amplitudes (see Reference 2 for more information). Source vector, $\boldsymbol{B}$, has the same structure. $\boldsymbol{B}$ is prescribed (corresponding, for example, to the output of a stator due to rotor wake input in an uncoupled environment) and $\boldsymbol{A}$ is to be found as a function of $\boldsymbol{B}$ by solving the linear system equations.

Coupling of the elements at the interface planes is specified in terms of the scattering matrix, $\boldsymbol{S}$, which is built up from modal reflection and transmission coefficients. In condensed form, the system equations are represented by

$$\boldsymbol{A} = \boldsymbol{SA} + \boldsymbol{B} \tag{1}$$

which is to say that the state vector elements are the sum of the parts from scattering, $\boldsymbol{SA}$, and directly from the source, $\boldsymbol{B}$. These equations are solved formally by

$$\boldsymbol{A} = (\boldsymbol{1} - \boldsymbol{S})^{-1}\boldsymbol{B} \tag{2}$$

Two major forms of noise output are computed from the state vector:

- Upstream and downstream propagating sound power levels are computed from $\boldsymbol{A}$ on a mode−by−mode basis. Power is calculated just upstream and just downstream of the noise source (defined in Figure 3 by interface plane 1 upstream, and interface plane 3 downstream).
- Outside far−field directivity is computed from the elements of $\boldsymbol{A}$. In this case, far−field directivity shapes are computed by the radiation codes with unit amplitude input and stored as part of the acoustic properties files. These directivities are then multiplied by $\boldsymbol{A}$ to get the far−field sound pressure level directivity.

TFaNS (Version 1.4) consists of the following computer codes:

- CUP3D Fan Noise Coupling Code Version 2.1 (Reference 2)
- SOURCE3D Rotor Wake/Stator Interaction Code Version 2.5 (Reference 3)
- Eversman Inlet Radiation code Version 3.0 (References 4, 5, 6)
- Eversman Aft Radiation code Version 3.1 (References 5, 6, 7)
- AWAKEN CFD/Measured Wake Postprocessor Version 1.0 (Reference 8)

3. GENERAL ORGANIZATION OF TFaNS

The organization of TFaNS is illustrated in Figure 4. This figure identifies the codes which comprise the system and how they interact with each other.

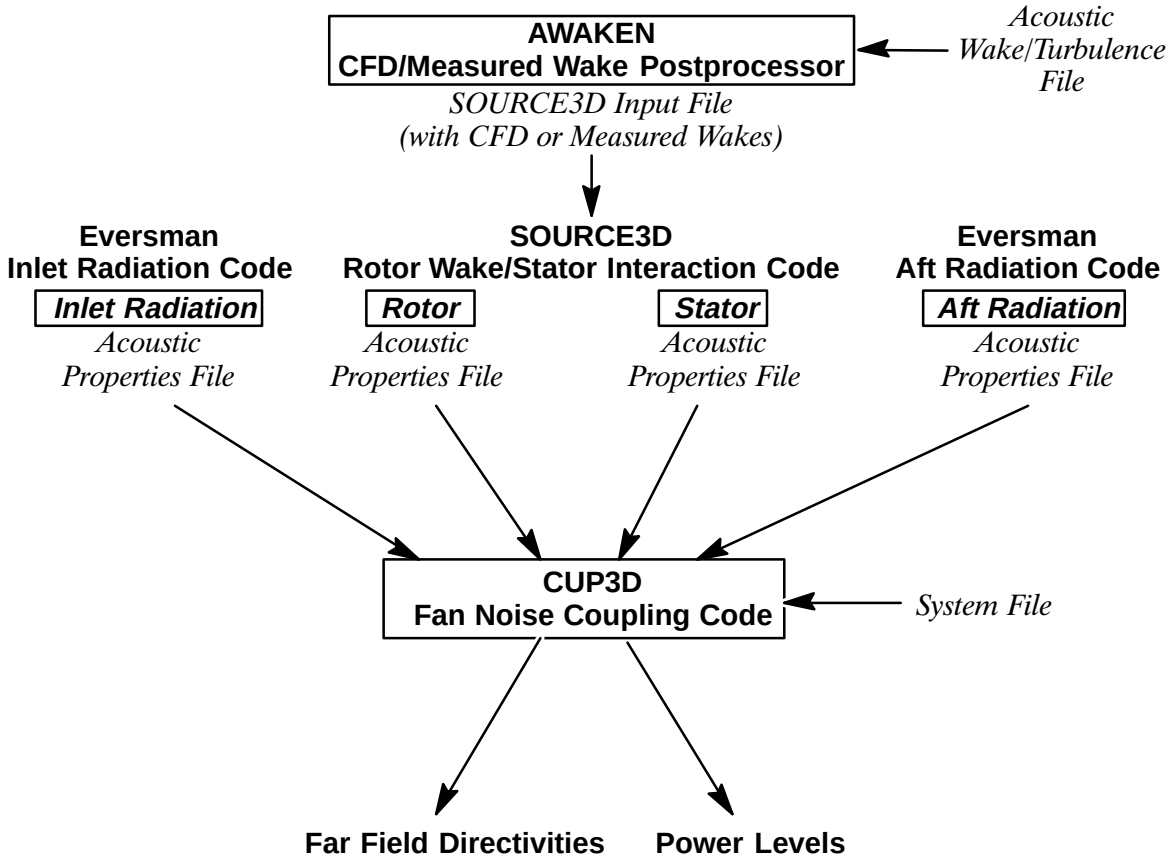

Figure 4: Organization of TFaNS Version 1.4

The central portion of the system is the CUP3D Fan Noise Coupling Code. This code reads Acoustic Properties Files which contain scattering (transmission and reflection) coefficients from other codes along with far−field directivity shapes and source vector information (e.g. noise from rotor wake/stator interaction). This information is used to form a system of linear equations which permit acoustic elements to reflect and transmit to each other. A System File is also input which determines the organization of the acoustic elements. Output from this code includes far−field directivities along with inlet and aft power levels.

The SOURCE3D Rotor Wake/Stator Interaction Code is a significantly extended and improved version of the V072 Rotor Wake/Stator Interaction Code (Reference 14 to 18). It has two functions within TFaNS: firstly, it calculates tone noise from a rotor wake/FEGV interaction and, secondly, it determines the scattering coefficients for the rotor and stator then outputs them to rotor and stator acoustic properties files (Figure 4) for use by CUP3D. This code can use CFD or measured wakes processed through the AWAKEN CFD/Measured Wake Postprocessor (as shown in Figure 4), or it can use its own internal semi−empirical wake model (as is used for this report).

The AWAKEN CFD/Measured Wake Postprocessor creates a SOURCE3D input file which contains upwash wake harmonic amplitudes calculated from CFD predictions or measured velocity data. CFD

or measured velocity information is obtained from the Acoustic Wake/Turbulence File which are generated either by a CFD code (or postprocessor) or during a engine/rig test program. This code is not being used in the evaluation of the system at this time, since its development and evaluation are being done under a different contract.

The Eversman inlet and aft radiation codes must be run if far−field directivities are required. These codes comprise three "modules". The first module creates a finite element mesh for the calculation. The second module calculates the potential steady flow using a method which divides the problem into three separate potential flow problems. This makes it possible to run the potential steady flow module once for a given nacelle geometry without knowledge of the duct flow conditions. Finally a radiation module, modified to interface with TFaNS, superimposes the potential steady flow solutions for a given set of duct flow conditions and calculates the far field radiation and scattering coefficients for a specified number of blade passing frequency (BPF) harmonics on a mode−by−mode basis.

4. SOUND POWER LEVEL EVALUATION OF TFaNS

Two geometries are used to evaluate this design system:

- Full−scale engine data−prediction comparisons are discussed first. These data correspond to those utilized in Reference 10 and examines the ability of TFaNS to model the rotor/stator coupling problem. For these cases, only rotor/stator coupling is performed and only sound power level comparisons with data are made. The inlet and the nozzle are not included in these calculations.
- The second geometry is that of the ADP 22" rig FAN1. This 18 blade, 45 vane model is a lower tip speed configuration where rotor/stator coupling was not expected to be important. For this case, Acoustic Properties files are generated for the inlet, rotor, stator, and nozzle. Coupling is then done using a number of combinations of these acoustic elements and the results are discussed. Sound power level predictions for this rig are presented in this section. Far−field directivity comparisons with data are presented in Section 5.

For both of these geometries the semi−empirical wake model in SOURCE3D is used with wake correlations from Reference 18. Note that for both of these geometries the fan wake/compressor inlet guide vane (IGV) interaction noise source was not predicted. This noise source is expected to contribute to inlet 2BPF and 3BPF in the full scale engine. It is not anticipated to be important to the ADP 22" rig due to the axial distance between the fan and the compressor IGV.

For this evaluation, Sections 4.1 and 4.2 will discuss data versus prediction comparisons for various levels of coupling of the inlet, rotor, stator, and nozzle, as they apply to the engine or rig configuration. While observations will be given, no conclusions from these observations will be discussed until Section 4.3. Section 4.3 will then present possible reasons why code results are as shown. Section 4.4 will then show some system experiments intended to improve the predictions where needed.

Also for this discussion we use the notation, $m = nB - kV$, where:

m = *circumferential mode order where m is positive in the direction of rotor rotation*
n = *harmonic of blade passing frequency*
B = *number of blades*
k = *any integer where* $-\infty < k < +\infty$
V = *number of vanes*

4.1 EVALUATION WITH FULL SCALE ENGINE DATA

In this section, the effects of rotor/stator coupling are evaluated using the full scale engine configurations from Reference 10. Acoustically treated data for these configurations were shown earlier in Figure 2 for three vane/blade ratios. Hardwall engine data are available for the lowest and highest vane/blade ratio configurations (vane/blade ratios = 1.9 and 2.2, respectively) in this figure and will be compared with predictions. No hardwall engine data are available for the middle vane/blade ratio.

As was stated previously, these full scale engine configurations display the wave reflection/mode trapping behavior discussed in References 1 and 10. The data were taken at an outdoor test stand with an inflow control device using standard test procedures.

The SOURCE3D rotor wake/stator interaction code was used to predict the rotor and stator noise. The CUP3D fan noise coupling code was then run to couple these elements assuming non−reflecting boundary conditions upstream of the fan and downstream of the FEGV. Coupled fan wake/FEGV

interaction predictions were made for the portion of the operating line where the fan relative Mach numbers used by the code remained subsonic consistent with the requirements of SOURCE3D. Rotor/stator coupled predictions included solid body swirl and flow turning for the acoustic calculations as described in Reference 3.

Separate uncoupled rotor wake/stator interaction noise predictions were also made without solid body swirl consistent with the original V072 code (References 14 to 18). For the uncoupled predictions, the $k = 0$ mode was not included in the inlet power level results, consistent with how V072 is presently run, because it is known to be cut off in the swirl region between the fan and the FEGV.

As in Reference 15, the semi−empirical tip vortex calculation was not included in the predictions. Only the semi−empirical wake calculation was used to drive the system.

As in V072, methods for defining certain geometry and performance parameters in SOURCE3D were developed. Reference 9 (the TFaNS user's manual) contains definitions for all the input parameters in SOURCE3D. We will now discuss briefly how some of these definitions were determined. After some evaluation it was determined that the stator stagger angles should be defined using the same definition as those used by V072 in Reference 15.

Defining the fan relative Mach number to be used in the rotor unsteady pressure distribution calculations is complicated by the rapid change of this quantity from the fan leading edge to the fan trailing edge. To handle this issue, the average of the fan leading edge and fan trailing edge relative Mach numbers is used. For consistency, the rotor stagger angles used by the code are defined by the angle the rotor chord makes with the tangential direction. This approximates the average metal angle of the fan at each radius. By running these average values, the fan can be run up to tip speeds where the fan leading edge relative Mach number is supersonic, but the average relative Mach number is subsonic.

SOURCE3D uses a solid body swirl approximation. After some investigation, the swirl velocity at 85% span was selected as the basis for the solid body swirl assumption. This spanwise location is the same as that used to investigate the wave reflection/mode trapping mechanism in Reference 10.

Figure 5 plots tone power level predictions for the 1.9 vane/blade ratio with hardwall data over a range of fan tip speeds. Coupled and uncoupled predictions are shown for the first three harmonics of BPF. Most of the data shown is hardwall data. Over, a portion of the speed range, acoustically treated data, corrected to hardwall conditions are shown (labelled "hardwalled" treated data). These data points are included for better evaluation of the rise in aft 3BPF power levels discussed previously.

We will first discuss the aft power level predictions (Figure 5d to Figure 5f), since they have tended to be the most stable when running in an uncoupled environment. Aft power level coupled predictions for this configuration show improved agreement with data over the uncoupled predictions. Aft 3BPF predictions are especially encouraging, as they predict the location of the significant power level rise seen in the data at about $850 - 900$ ft/sec fan tip speed. Aft 2BPF coupled predictions also compare better with data than the uncoupled results. BPF coupled predictions show that this tone is not dominated by the rotor wake/stator interaction tone noise source but is dominated instead by other noise sources.

With reference to Figure 5f, we will now discuss in greater detail the 3BPF power level rise observed in the coupled predictions. In Reference 10, a simple thin annulus theoretical model was used which limited the analysis to only the first radial mode order of each circumferential mode. For BPF, only the $m = B - V$ circumferential mode (i.e. $k = 1$) is propagating forward in the swirl region between the fan and the FEGV's. Thus, this simple model found that the first propagating BPF radial mode ($\mu = 0$) was what caused the significant "mode trapping" and related rise in the aft 3BPF predictions.

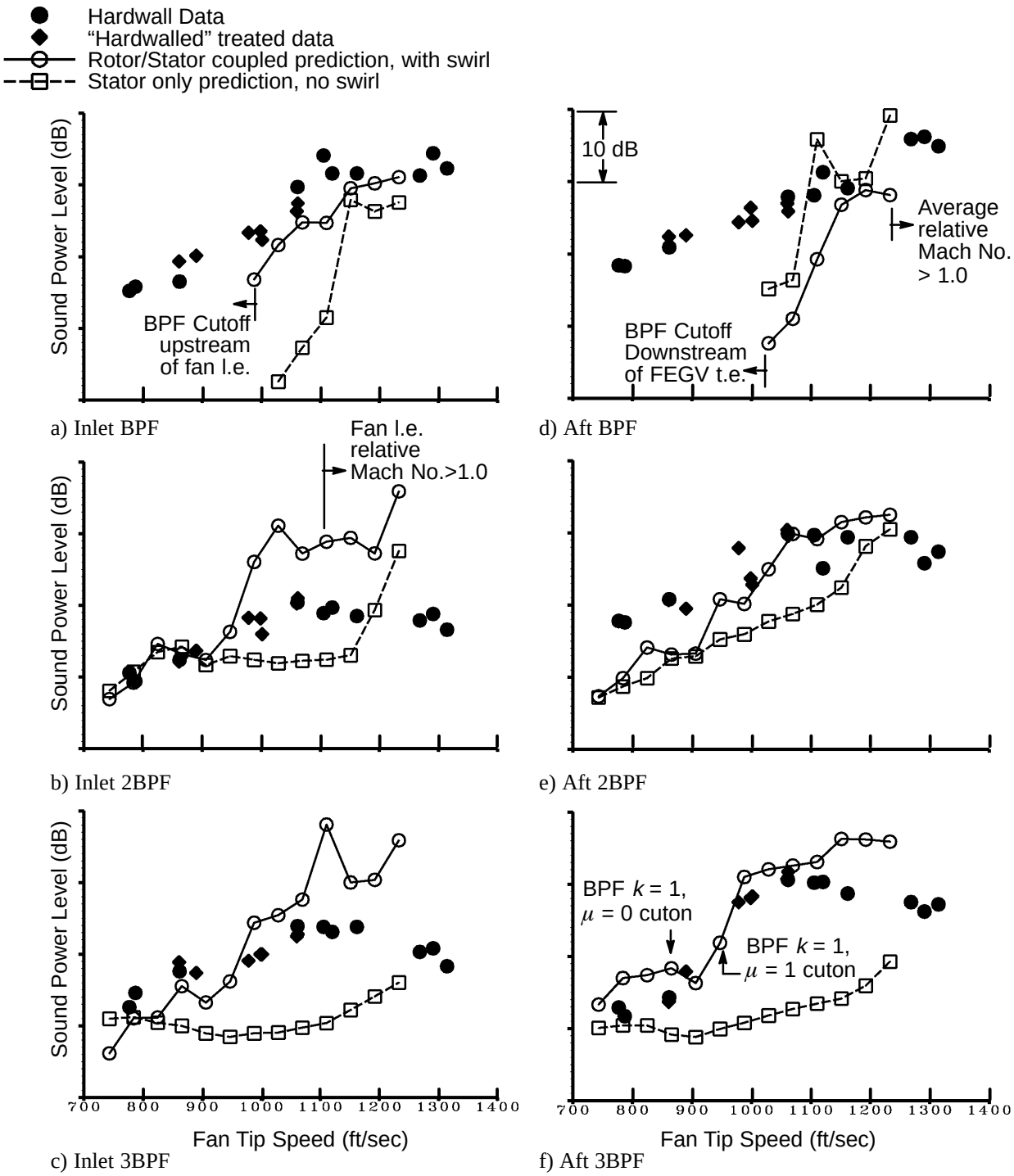

Figure 5: Full Scale Engine Tone Noise Data vs. Prediction, 1.9 Vane/Blade Ratio

Analysis of the SOURCE3D/CUP3D coupled predictions indicates that this first radial mode cuts on at about 850 ft/sec in the swirl region between the fan and the FEGV's. Predictions however, do not show a significant rise until the second radial mode ($\mu = 1$) cuts on at about 950 ft/sec. This is because the amplitude of the first radial mode order at BPF, predicted by the rotor wake/stator interaction noise source, is too low as it propagates forward from the stator to have a significant impact on aft 3BPF. It is not until this second radial mode order cuts on at BPF, in the swirl region between the fan

and the FEGV, that coupling causes a significant rise in aft 3BPF power levels. This is reflected in the aft predictions for both 2BPF and 3BPF.

In this engine, inlet 3BPF noise is expected be dominated by rotor wake/compressor IGV interaction noise (as shown in Reference 15). This noise source is also expected to contribute to inlet 2BPF noise. However, inlet 2BPF and 3BPF power level predictions in Figure 5b and Figure 5c also show evidence of coupling. This coupling appears to be reasonable up until about 1000 ft/sec fan tip speed. Above this speed coupling is overpredicted by the system, especially for inlet 2BPF. Some of this overprediction may be in part due to the fact that the fan leading edge relative Mach number is greater than one for the last four predicted speeds (see Figure 5). This means that shocks, whose effect is not modelled in this analysis, have likely formed on the fan.

In addition, waves propagating forward through the rotor are impacted by higher reduced frequencies (in the rotating reference frame) than those seen in the stator. Appendix I discusses computational experiments that have been performed using the Smith code (Reference 13) to investigate the effect of these frequencies on the results and to develop chordwise integration station criteria for SOURCE3D. This 2D code showed that predicting forward propagating noise at these high speeds is extremely difficult. Aft noise, however, seems to give more stable results at the high speeds in 2D. These 2D results are consistent with the predictions in Figure 5.

Inlet BPF power levels (Figure 5a) also show evidence of coupling when BPF is cut on. Results appear to follow the data, though the high tip speeds of the rotor where these were run may make these predictions somewhat questionable.

Figure 6 shows tone noise predictions versus hardwall data for the 2.2 vane/blade ratio case in Figure 2. These noise predictions follow the same format used in the previous figure. Aft power level predictions (Figure 6d to Figure 6f) also compare better with data for the coupled case than the uncoupled case although aft 2BPF predictions show little effect of coupling. Aft 3BPF results show an effect of coupling and better results versus data. However, they do not show the sudden rise in 3BPF seen in Figure 2. This seems to be once again due to low predicted levels for the stator generated BPF $k = 1, \mu = 0$ mode. Aft BPF noise is predicted to be cut on over a portion of the speed range. This tone noise is due to the appearance of the $k = 0$ mode (i.e. $m = B - 0V$ mode) in the results.

Inlet 2BPF and 3BPF coupled predictions (Figure 6b and Figure 6c) for this vane/blade ratio show variable comparisons at low speeds. Inlet 2BPF noise is well predicted at low speeds while inlet 3BPF power levels are significantly underpredicted. Thus, inlet 3BPF low speed results are consistent with the expectation that rotor wake/compressor IGV interaction noise dominates this tone.

At high fan tip speeds, when the fan leading edge relative Mach number becomes greater than one, inlet 2BPF and 3BPF are significantly overpredicted much like the 1.9 vane/blade ratio configuration. This overprediction occurs when the rotor is supersonic. Thus shocks, not accounted for by TFaNS, and high rotor reduced frequencies seem like the most likely explanation for why the noise is overpredicted. Inlet BPF power levels (Figure 6a) do not cut on until high speeds, and even then are predicted to have no real impact on the resulting noise.

Also impacting on these high speed predictions for the 1.9 and 2.2 vane/blade ratio configurations are the rotor predicted transmission coefficients may be too large for some modes. This issue is further discussed in the following sections.

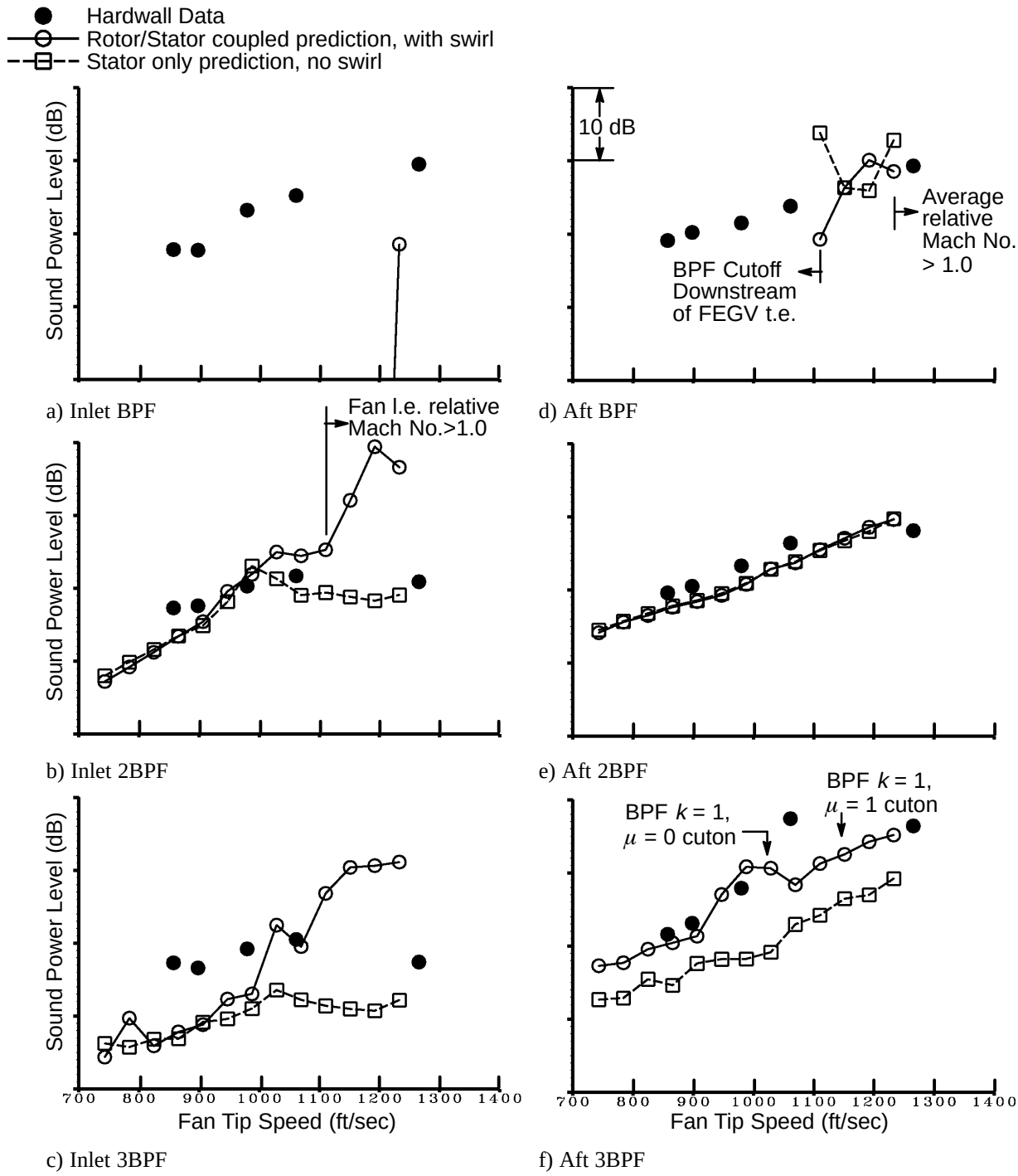

Figure 6: Full Scale Engine Tone Noise Data vs. Prediction, 2.2 Vane/Blade Ratio

4.2 EVALUATION WITH ADP 22” RIG FAN1 DATA

The previous section presented results for coupled rotors and stators without including the effects of an inlet and nozzle. This section evaluates TFaNS ability to predict sound power levels for a coupled inlet, rotor, stator, and nozzle configuration. Data from the ADP 22” fan FAN1 rig are used for this

portion of the evaluation. Far−field sound pressure level directivity data−prediction comparisons for this rig are discussed in Section 5.

Test data for the ADP 22" rig were obtained at the NASA Lewis 9' x 15' low speed wind tunnel. The fan has 18 blades and 45 vanes and runs at a top fan tip speed of 950 ft/sec. The rig includes a rotor, a FEGV and a core duct (see Figure 7). Data were obtained at a constant sideline distance from the model with a microphone traverse and were postprocessed to a constant far−field radius from the rig. Tones were calculated by subtracting the broadband from the tone levels. Note that BPF is cut off over the entire speed range in this rig.

Figure 7 shows how TFaNS models the ADP 22" Rig FAN1 rig. Dark lines indicate geometry modifications to deal with computer code limitations. The inlet and nozzle geometries were not changed in the radiation codes except that for the aft radiation code, the centerbody radius was gradually reduced to zero sufficiently far from the nozzle exit so as not to impact on aft radiated noise. This geometry modification was required by the aft radiation code in order for it to run correctly. The axial location of the centerbody modification was determined by experimenting with the aft radiation code using this geometry.

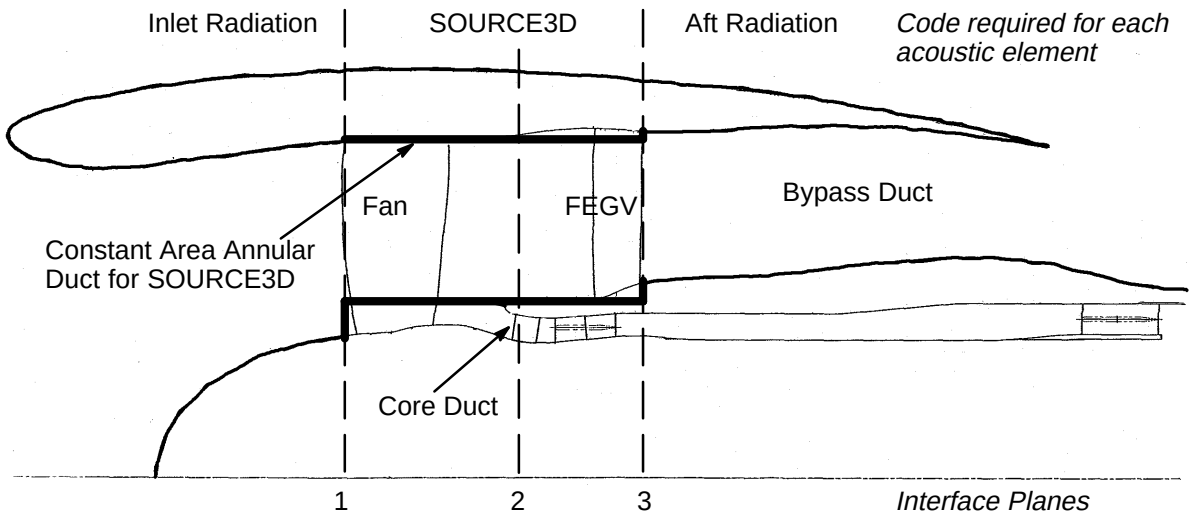

Figure 7: ADP 22" Rig FAN1 Cross Section as Modelled by TFaNS

Also on this chart are the interface plane numbers shown consistent with Figure 3 and the codes which are run to create Acoustic Properties Files for each of the acoustic elements. Note that from interface plane 1 to interface plane 3 a constant area annular duct is defined which permits SOURCE3D to do its calculations. Interface plane 1 is shown as the input plane for the inlet radiation code while interface plane 3 is shown as the input plane for the aft radiation code. Note that actual nacelle geometry is used to perform the two radiation code calculations. This creates some incompatibility with the duct modes between the radiation codes and SOURCE3D. This incompatibility was accepted because modifying the nacelle geometry to be consistent with SOURCE3D would noticeably change the steady background flow for the radiation calculations thus having an impact on the noise predictions.

Figure 8 compares sound power level predictions using TFaNS with three acoustic element combinations. They are listed here from the least sophisticated method of running TFaNS to the most sophisticated method. The triangular symbols show predictions for a stator only prediction without swirl. This is essentially a V072 Rotor Wake/Stator Interaction Code prediction (References 14 to 18).

The square symbols show a rotor/stator coupled prediction with swirl and turning consistent with the previous section. Finally, the circular symbols show "fully coupled" predictions which include an inlet, rotor, stator, and nozzle with swirl and turning.

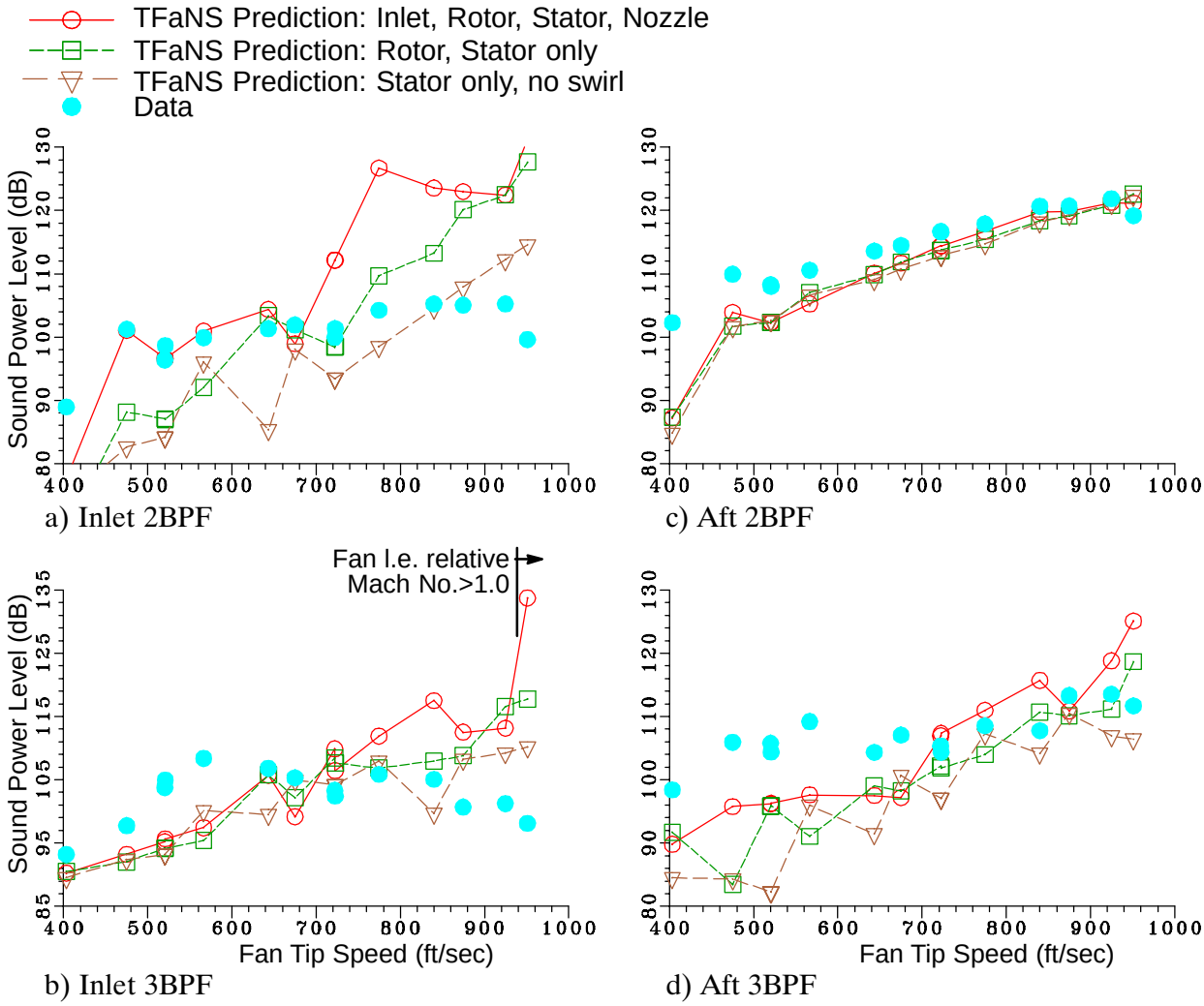

Figure 8: ADP 22" Rig FAN1 Predictions vs. Data with different levels of coupling

Aft 2BPF noise for all of these predictions tend to compare well with data. Predictions are quite similar to each other indicating that the effect of coupling is small. Aft 3BPF does show some changes with coupling. But mostly these effects are comparatively small. With the exception of the last two speeds, the fully coupled predictions are the closest to the data, though all the predictions tend to underpredict 3BPF at tip speeds below about 650 ft/sec. This may, in part, be due to the wake model (see Section 4.3).

Inlet 3BPF noise shows little coupling below about 700 ft/sec tip speed. Above this speed, the rotor/stator coupled predictions and the fully coupled predictions begin to overpredict the data. Inlet 3BPF tends to be underpredicted below about 650 ft/sec tip speed. As with aft 3BPF results, this may be partially due to the wake model.

Inlet 2BPF predictions show increasing levels of coupling which tend to improve the level of data−prediction agreement below about 700 ft/sec tip speed. Above this speed, increasing the amount

of coupling tends to predict noise increases that are inconsistent with the data. In addition, the predicted shape of inlet 2BPF versus speed is not predicted correctly by any of the alternative calculations.

The remainder of this section will focus on gaining a better understanding of the inlet 2BPF and 3BPF noise prediction behavior. To further analyze these results, coupled predictions are made which exclude either the inlet or the nozzle. The purpose of this exercise is to see if there is a considerable effect of the inlet over the nozzle in determining the coupling behavior. Figure 9 shows predictions for the fully coupled case, inlet/rotor/stator coupled case (no nozzle included), and rotor/stator/nozzle coupled case (no inlet included). Once again, the largest effects seem to occur for the inlet 2BPF predictions. Thus, inlet 2BPF results will be further discussed.

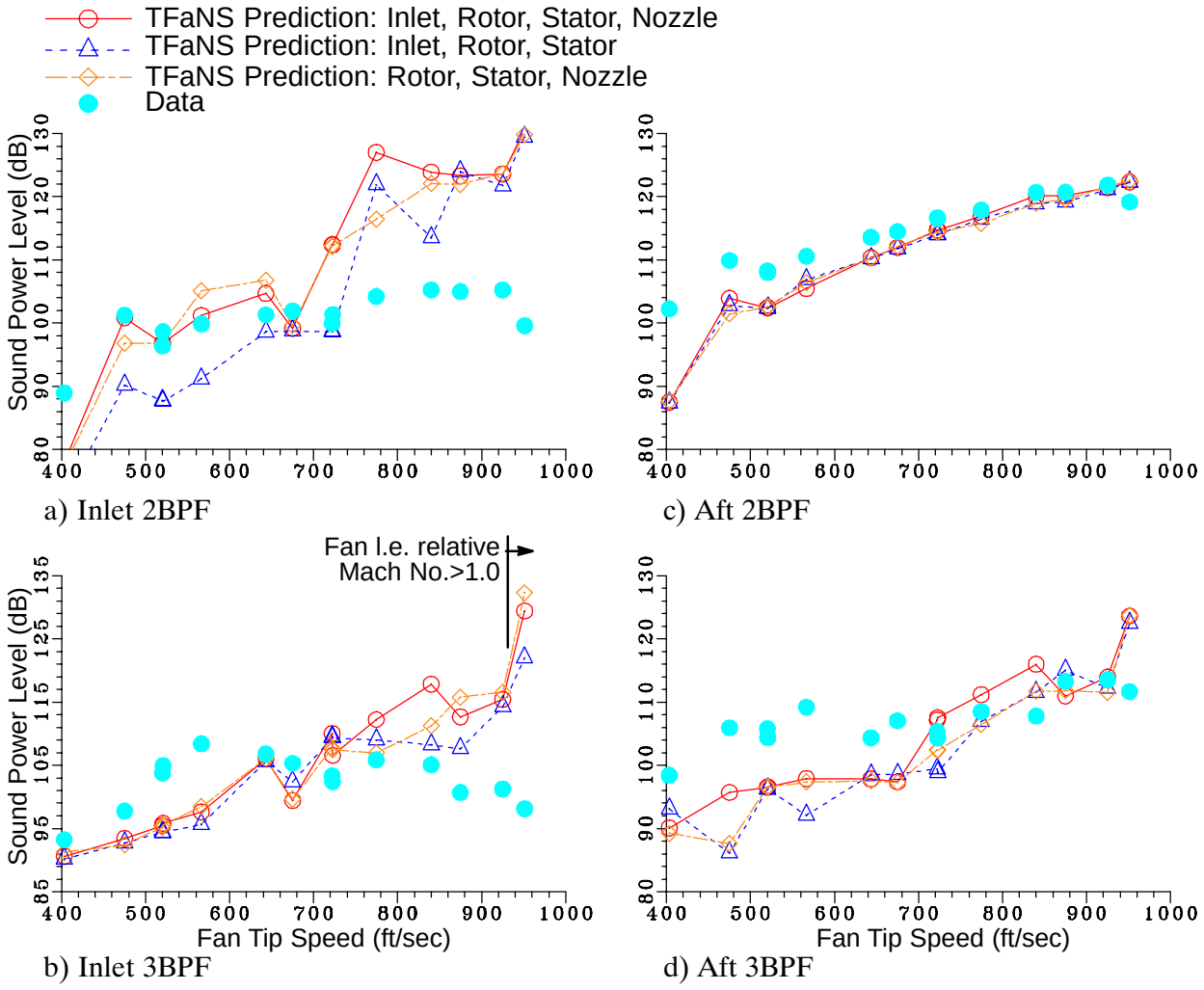

Figure 9: ADP 22" Rig FAN1 Predictions vs. Data with various levels of inlet or nozzle coupling

Figure 10 shows inlet 2BPF sound power levels versus fan tip speed in more detail. It includes all the same plots as in Figure 9 as well as the rotor/stator coupled predictions. The stator only prediction without swirl, shown in Figure 8, is also included for reference. We will now further discuss this figure by splitting the analysis into two parts: low speed results (i.e. 475 − 643 ft/sec tip speeds) and high speed results (i.e. 723 − 840 ft/sec tip speeds). Since 675 ft/sec shows little effect of coupling, it will not be discussed in further detail here. All comparisons below are made relative to the rotor/stator coupled predictions.

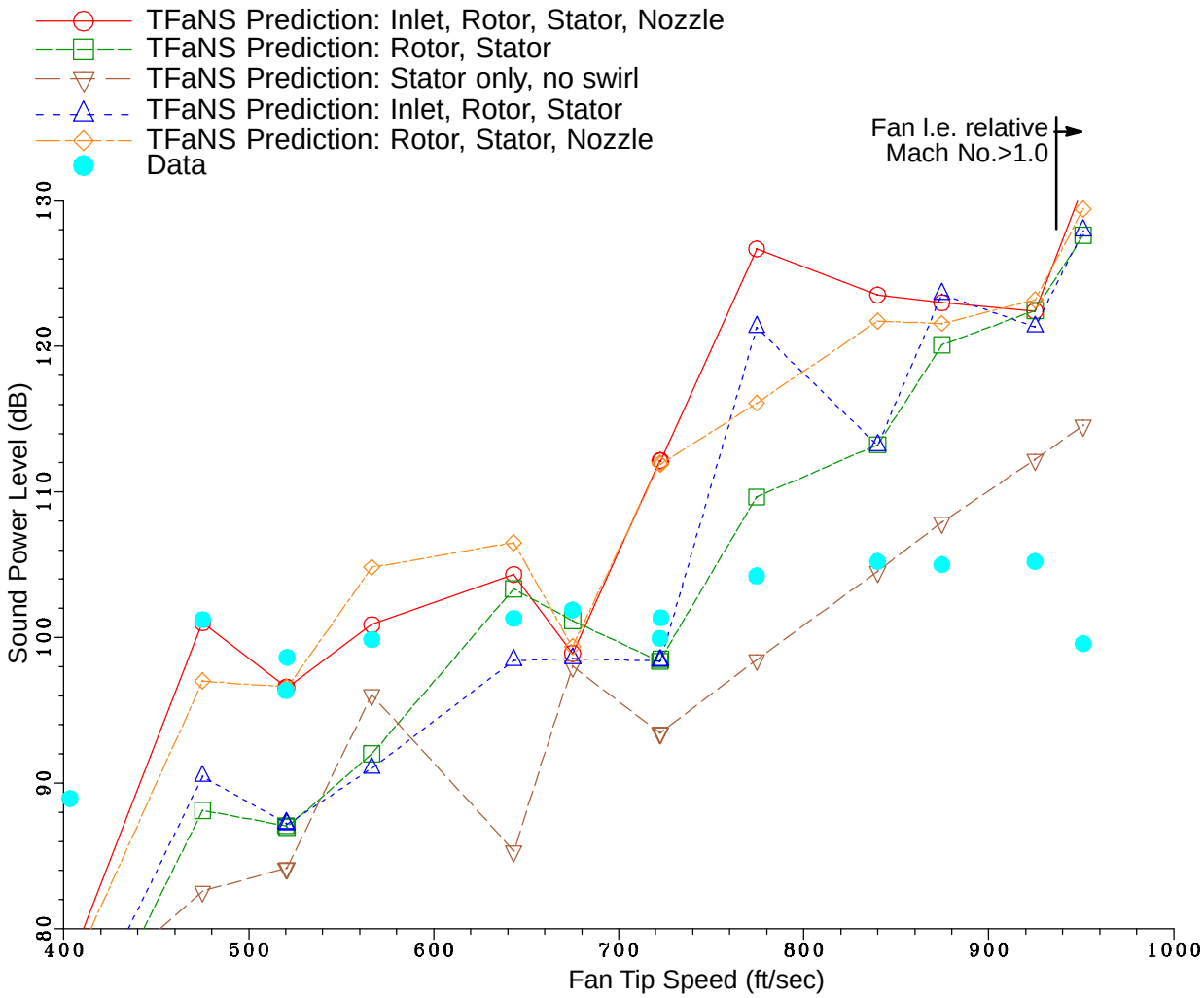

Figure 10: ADP 22" Rig FAN1 Inlet 2BPF Predictions vs. Data with various levels of coupling

At the low speeds, including the inlet and nozzle tends to significantly improve how well predictions compare with data. Based on the rotor/stator/nozzle predictions, the addition of the nozzle has the largest impact on the results. The addition of an inlet tends to then improve the predictions to better match the data. The effect of the nozzle on inlet noise appears to be due, in part, to the fact that inlet 2BPF data is about 10dB lower than aft 2BPF data over the entire speed range (see Figure 9). Thus reflections from the nozzle will more likely effect the inlet predictions than reflections from the inlet impacting on aft results.

To better understand the results, we will now examine the reflection coefficients from the inlet and aft radiation code predictions. Table I shows pressure mode reflection coefficient magnitudes (in decibels) predicted by the inlet and aft radiation codes. In order for this table to be useful, the "input" and "output" modes need to be important to the solution. Thus, in this table, "input" (m, μ) modes correspond to modes found to be important in rotor/stator coupled predictions at the rotor leading edge (l.e.) for forward propagating modes and at the stator trailing edge (t.e.) for aft propagating modes. The "output" (m', μ') modes correspond to modes, predicted to be important in the fully coupled predictions. In this table, the dominant "output" modes are marked. During this discussion, m = circumferential mode order and μ = Radial mode order. (m', μ') refers to the mode which is

being scattered into. Note that, except at 566 ft/sec tip speed, the nozzle pressure reflection coefficients are less than −5.0dB for the dominant modes.

TABLE I: 2BPF REFLECTION COEFFICIENTS AT FOUR LOW SPEEDS

Fan Tip Speed	Input Mode *m, μ*	Output Mode *m', μ'*	Magnitude of Pressure Mode Amplitude Reflection Coefficient		Input mode Dominates inlet Mode Power Level for Fully Coupled Prediction?
			Inlet Reflection, fan l.e. (dB)	Nozzle Reflection, FEGV t.e. (dB)	
475 ft/sec	−9,1	−9,1	−1.6	−8.2	YES
	−9,0	−9,1	−19.2	−8.9	NO
521 ft/sec	−9,1	−9,1	−33.1	−13.9	YES
566 ft/sec	−9,2	−9,2	−1.9	1.7	YES
643 ft/sec	−9,3	−9,3	−2.4	Cut off	NO (dominant for rotor/stator only coupling)
	−9,2	−9,2	−30.5	−13.2	YES
	−9,1	−9,2	−34.0	−13.2	NO
	−9,0	−9,2	−40.9	−5.5	some importance
	−9,2	−9,0	−46.0	−12.8	YES
	−9,1	−9,0	−40.9	−19.2	NO
	−9,0	−9,0	−46.0	−12.0	some importance

We will now discuss each speed separately to better understand the results. At 475 ft/sec tip speed, at the stator, inlet 2BPF noise data is about 10dB lower than aft 2BPF noise data. For rotor/stator coupled predictions, this inlet to aft difference is predicted to be about 14dB (Figure 8). Thus reflection coefficients of −8.0 to −9.0dB from the nozzle (Table I) may have an important impact on inlet noise.

At 521 ft/sec, inlet 2BPF predictions for the fully coupled system are dominated by the (−9,1) mode and thus seem to be due to the reflections off the nozzle due to the much higher aft noise levels relative to the inlet noise. Also of interest, the (−9,2) mode (where $k = 1$) is trapped between the rotor and stator. An analysis of the modal results in the rotor/stator coupled predictions (shown in Figure 8) indicates that this trapped mode is reflected into aft 3BPF noise as a (9,2) mode (where $k = 1$).

At 566 ft/sec tip speed, the (−9,2) mode is cut on from the fan l.e. to the FEGV t.e. (Cutoff ratio, $\xi \approx 1.05$ at the fan l.e. and the FEGV t.e.). As the mode makes its way into the inlet or nozzle, it becomes cut off, thus causing this mode to be trapped. But if we look at Figure 10, we notice that just adding the nozzle onto the acoustic system causes a noise rise out the inlet. This makes sense since the reflection coefficient shown in Table I is quite high for the nozzle, thus causing the noise to reflect back through the inlet. The inlet, however, does not produce the same effect on aft 2BPF noise as is seen in Figure 9 since aft noise is so much higher than inlet noise.

Also note that at 566 ft/sec the nozzle reflection coefficient in Table I is greater than 0dB indicating that the reflected pressure magnitude is higher than the incident magnitude. This is reasonable since these are *pressure* reflection coefficients for a downstream going pressure wave being reflected into an upstream going pressure wave. For power to be conserved, it is the *power* reflection coefficients that must be less than 0dB. The derivation of the pressure reflection coefficients for the radiation codes may be found in Reference 2.

Predictions at 643 ft/sec tip speed are perhaps the most complicated of the low speed results. Fully coupled inlet 2BPF predictions are quite similar to the rotor/stator coupled results. However, predictions without an inlet or without a nozzle show some considerable changes which are worth exploring to better understand the solutions.

Coupled predictions using inlet/rotor/stator acoustic elements are lower than the rotor/stator coupled results. This is due to the fact that rotor/stator coupled noise source has a dominant $(-9,3)$ mode which is very near cutoff ($\xi = 1.004$) at the fan l.e. and is cut off at the FEGV t.e. When the inlet is added to the coupling, the inlet cuts off this mode, thus reducing the total inlet power.

Adding a nozzle to the system causes the noise to rise back up as the $(-9,2)$ mode becomes dominant and the $(-9,0)$ mode becomes important. Table I shows that the $(-9,0)$ and $(-9,2)$ mode nozzle reflection coefficients appear too low to have a significant impact on the inlet noise results. Note that the aft 2BPF prediction at the stator t.e. is only 7dB higher than inlet 2BPF at the rotor l.e. for a rotor/stator coupled prediction (Figure 8). Further investigation finds that the aft radiated $(-9,2)$ mode power level is 26 dB higher than the inlet radiated $(-9,2)$ mode power level for inlet/rotor/stator coupled predictions. Thus, even though the nozzle reflection coefficient for this mode is -13.2 dB, it is still causes reflected 2BPF noise which is considerably higher than the inlet noise. This causes inlet noise to rise and making the $(-9,2)$ mode dominant out the inlet. Also, the $(-9,0)$ mode, which is much lower out the inlet than the aft, appears to be impacted by the scattering of the $(-9,1)$ mode into the $(-9,0)$ mode.

In summary, for inlet 2BPF at the low speeds, rotor/stator coupled predictions compare slightly better to the data than stator only, no swirl (i.e. V072 type) predictions. Both predictions underpredict the data, however. The discussion above shows that, at these low speeds, the inlet and the nozzle must be included in the model to effectively predict inlet 2BPF sound power levels for this rig.

The next part of this discussion will concentrate on the higher speeds. The 675 ft/sec tip speed result is skipped in this discussion since its results for inlet 2BPF power levels are quite similar for the various levels of coupling. Above 723 ft/sec tip speed, coupled predictions tend to overpredict the data as is shown in Figure 10.

Using Figure 10, we will now discuss how predictions with various levels of coupling compare to data and to each other. The rotor/stator coupled prediction is about 10dB higher than for the stator alone, no swirl prediction. Adding the rotor improves agreement with data at the low speeds, but worsens agreement at the high speeds. When the nozzle is added to the coupling, the system overpredicts the high speed data further except at the three highest speeds where rotor/stator coupled predictions and rotor/stator/nozzle coupled predictions are similar. These results show that the rotor has an important impact on the total predicted power levels (shown in Figure 10) at the high speeds. Aft radiation code coupling then further exaggerate the predictions. At the very high speeds, only the rotor/stator coupling has a significant impact on the results.

To investigate the higher speed overprediction, Table II is used. This table shows inlet and nozzle reflection coefficients for three speeds where adding the nozzle significantly changes the predictions. Definitions used in this table are the same as those used in Table I. Table II shows that while inlet radiation reflection coefficients are -5.8dB or less, aft radiation code reflection coefficients are 0.9dB or higher for the dominant inlet sound power level mode.

Note that for all the speeds in Table II, the dominant inlet noise mode is cut off somewhere in the nozzle, thus causing the high nozzle reflection coefficients. Also, at these high speeds, the aft radiation code is having some significant difficulty predicting the far$-$field. According to Reference 19, because of the size of the noise source (defined as the nozzle plus the shear layer) the acoustic waves at the

interface between the standard finite element region and the wave envelope region are not lined up correctly with the wave envelope elements. This can cause reflections back into the standard finite element region, possibly causing reflections back into the duct. These two issues may impact on the nozzle reflection coefficients in Table II.

TABLE II: 2BPF REFLECTION COEFFICIENTS AT THREE HIGH SPEEDS

Fan Tip Speed	Input Mode m, μ	Output Mode m', μ'	Magnitude of Pressure Mode Amplitude Reflection Coefficient		Input mode Dominates inlet Mode Power Level for Fully Coupled Prediction?
			Inlet Reflection, fan l.e. (dB)	Nozzle Reflection, FEGV t.e. (dB)	
723 ft/sec	−9,3	−9,3	−24.4	2.3	YES
775 ft/sec	−9,4	−9,4	−5.8	Cut off	YES
	−9,3	−9,3	−20.9	3.3	NO (5 dB lower than −9,4 mode)
840 ft/sec	−9,4	−9,4	−19.2	0.9	YES

Also impacting on these high speed predictions are the rotor predicted transmission coefficients which appear to be too large for some modes. This causes the high reflections from the nozzle to pass through the rotor, predicting high inlet tone noise which is much higher than the data. This difficulty may be due to either high frequencies or high fan relative Mach numbers which effect the system's ability to predict inlet noise. This concept will be further discussed below and in the following sections.

For the higher speeds, only the prediction at 775 ft/sec tip speed will be discussed in detail. The system results show that for this speed, the (−9,4) mode is cut off at the FEGV t.e. and in the inlet so that this mode is trapped and cannot exit the nozzle. This increases the overall predicted power level of the inlet 2BPF tone for the rotor/stator coupled prediction. For this tip speed, inlet 2BPF is increased even more by coupling to the inlet. This appears to be due to the (−9,4) mode reflecting back from the inlet into rotor and interacting with the rotor. Note that inlet/rotor/stator coupled inlet 2BPF power level predictions are higher than the aft predictions as is shown in Figure 9 implying that inlet reflections are important for this case. Calculations also show that the fully coupled and inlet/rotor/stator inlet 2BPF predictions are dominated by the (−9,4) noise whereas the rotor/stator/nozzle predictions are dominated by the (−9,3) mode. While the mode trapping is predicted to impact on the noise levels at this speed, this effect well overpredicts the data. This result points towards the possibility that at the high speeds the 2D unsteady pressure distribution calculation combined with the 3D acoustics in SOURCE3D are causing incorrect transmission coefficients to be calculated for the rotor.

4.3 PRELIMINARY CONCLUSIONS FROM THE TFaNS POWER LEVEL EVALUATION

Results of this sound power level evaluation of TFaNS with full scale engine and the ADP 22" rig data show that the effect of coupling varies with the strength of various incident modes in the system. Full scale engine predictions show a strong effect of rotor/stator coupling when BPF cuts on in the swirl region between the fan and the FEGV's. The ADP 22" rig, conversely shows that rotor/stator coupling has a limited impact on the predictions. This may be due to the fact that in this rig BPF is cut off so that there are few strong inlet propagating modes to excite the system. However, when a nozzle is added to the problem, inlet 2BPF predictions change significantly. Thus, the results of this power level evaluation show that coupling of the inlet, rotor, stator or nozzle are important to the prediction of fan tone noise.

Sound power level calculations, when compared to data for a full scale engine and the ADP 22" rig, show that TFaNS (either in the form of rotor/stator coupling or inlet/rotor/stator/nozzle coupling) predicts aft noise as well or better than a stator alone, no swirl calculation (i.e. V072 rotor wake/stator interaction code type prediction). This is especially true when significant coupling occurs. TFaNS inlet noise is also as well or better predicted than a stator alone calculation below about 750 ft/sec tip speed for the ADP 22" rig and below about 1000 ft/sec for the full scale engine. Above these speeds, TFaNS inlet noise is predicted more poorly than for a stator alone, no swirl calculation. The discussion below gives possible reasons why inlet noise is poorly predicted at these higher tip speeds.

TFaNS overpredicts inlet noise at high speeds even when only rotor/stator coupling is used. The addition of an inlet and/or nozzle (especially a nozzle) further increases the predicted noise. This indicates that rotor and nozzle scattering issues are likely causing some of the high noise predictions. Based on these observations, the following possible reasons are given to explain why the system is having difficulty predicting the higher speed inlet radiated noise:

- 2D aerodynamics combined with 3D acoustics cause scattering coefficient inaccuracies. Note that the SOURCE3D rotor wake/stator interaction code models the unsteady pressure distribution in 2D and couples it to a 3D acoustic calculation. These two calculations each have their own requirements and limitations and are not totally consistent with each other. The inaccuracies resulting from this approximation do not appear to be particularly important to the aft radiated noise or the inlet radiated noise at low speeds. However, as frequencies become higher on the rotor at high speeds, inaccuracies in the predicted rotor transmission loss appear to be important to inlet radiated noise. Since rotor/stator coupled results show the rotor to be important to the predictions, this issue is likely to be important on the rotor where high speeds result in high reduced frequencies in the rotor reference frame and high fan relative Mach numbers.
- The aft radiation code has difficulties predicting noise as the reduced frequency is increased. These problems are seen when predicted far−field directivities are no longer relatively smooth continuous curves, as is shown in Section 5. Predicted far−field discontinuities are concentrated forward of the nozzle and gradually moves further aft as the reduced frequency increases. It has been suggested (Reference 19) that this may be due to the large size of the noise source (which includes the shear layer) as perceived by the code. This may lead to a non−smooth interface at the boundary between the standard finite elements and the wave envelope elements causing reflections back into the standard finite element regions. As a result, reflection coefficients calculated by this code could be affected, thus impacting on the final noise predictions. This behavior may partially explain why, when the nozzle is added to the ADP 22" rig high speed predictions, the inlet 2BPF noise was significantly higher than the rotor/stator coupled results.

  An alternate explanation for this issue could be that the nozzle reflection coefficients are reasonable, but the rotor transmission coefficients being calculated by SOURCE3D are too high at high speeds, giving high inlet noise. Reducing the transmission coefficients would reduce the impact of the nozzle reflection coefficients on the inlet noise. This is consistent with the 2D aerodynamic/3D acoustic issue discussed above.
- Unsteady pressure distributions are calculated using a 2D subsonic, linearized, flat plate cascade model. This model relies on a panel method which has frequency limitations when the number of panels is increased to respond to the higher reduced frequencies or higher incoming Mach numbers. This limitation was found during the development of rotor chordwise integration station criteria for the SOURCE3D Rotor Wake/Stator interaction code (see Appendix I). Thus pressure distributions, especially on the rotor at high speeds where the subsonic, linearized assumption is beginning to be challenged, do not necessarily reflect the actual distributions on the cascade. This may lead to an incorrect solution, especially in the inlet where the acoustic reduced frequencies become quite high as the relative (fan blade fixed) Mach numbers rise.

These three issues appear to be the most likely reasons for poor data−prediction agreement in the high speed inlet radiated noise.

Other approximations in TFaNS which may impact on the results include:

- Solid body swirl, used only in the acoustic calculations, may not be representative enough of the real flow to calculate consistent, correct solutions.
- The actuator disk model may not be indicative enough of the real flow turning to get consistent solutions. This relates back to the unsteady pressure distribution issue discussed above.
- Hub to tip ratios for the inlet, rotor/stator, and nozzle are all different. This means that the mode eigenfunctions (mode shapes) do not match exactly at the TFaNS interface planes. This incompatibility may be an issue for certain conditions where inlet and/or nozzle acoustic elements are used, especially in the inlet, where the hub to tip ratio changes the most (due to our not including the compressor IGV duct in the SOURCE3D predictions).

  Note that "adjusting" the inlet, rotor/stator and nozzle hub to tip ratios so that they did match would have a significant impact on the steady flow in the inlet and nozzle thus impacting on the noise. It would also make using the radiation codes more difficult because each nacelle geometry would need to be changed from its real geometry.

These other assumptions appear to be secondary relative to the 2D aerodynamic/3D acoustic interface, aft radiation code, and the rotor/stator pressure distribution calculation issues.

The low speed inlet and aft 3BPF predictions for the ADP 22" rig case are lower than the data. There are now wake measurements for the ADP 22" rig FAN1 which indicate that this underprediction may be due, in part, to the wake model in SOURCE3D. This code presently uses a wake model where the wake width and velocity deficit are calculated using correlations of high tip speed fan rig data at the rig design speed. At low speeds (off design) these wakes may not always be representative of the real wakes coming off a fan. This issue will be covered further in a future report.

To better understand the impact of the rotor pressure distribution and the 2D aerodynamic/3D acoustic interface on the results, the ADP 22" rig predictions are used for further analysis and are presented in the next section.

4.4 INVESTIGATING THE EFFECTS OF THE 2D AERODYNAMIC/3D ACOUSTIC INTERFACE IN SOURCE3D

As a result of the analyses in the previous sections, it was hypothesized that the ADP 22" rig and full scale engine noise at the high speeds could be overpredicted because the panel method used to calculate the unsteady pressure distribution on the rotor was reaching its frequency limit. Appendix I, which discusses the development of chordwise integration station criteria for the rotor and stator, shows a low reduced frequency case (Appendix I, Figure 9c) where adding panels causes the panel method to break down. This same problem has been observed at high reduced frequencies where using the required high number of panels for the unsteady pressure distribution caused the calculation to break down. In addition, during the work which was needed to create the rotor chordwise integration station criteria, it was found that the panel method in the Smith code (Reference 13) could not resolve 2D upstream propagating pressure waves for high frequency or high Mach number cases. However, when rotor pressure distributions were investigated for the ADP 22" rig at 840 ft/sec tip speed, no such problem was found. Thus this problem appears to be limited to higher rotational speed rotors (e.g. the full scale engine).

Consequently, this investigation focuses on incompatibility of the 2D aerodynamic calculations with the 3D acoustic calculations in the SOURCE3D rotor wake/stator interaction code. In this code the

unsteady pressure distributions on the rotor and stator are calculated assuming small perturbations of a mean flow into a 2D cascade of flat plates. This 2D aerodynamic theory is then coupled to a 3D acoustic problem which does its calculations by coupling the unsteady pressures from the 2D cascade to acoustic modes of a constant area annular duct with mean axial flow and solid body swirl. These two calculations are somewhat incompatible with each other but have been successfully used in the V072 rotor wake/stator interaction code to calculate noise from an isolated stator. SOURCE3D uses this method to calculate the rotor wake/stator interaction noise solution, and scattering coefficients from the rotor and stator. The compatibility of the 2D aerodynamics coupled with the 3D acoustics appears to be an issue for high speed calculations using SOURCE3D.

At 840 ft/sec tip speed, the rotor scattering coefficient mode magnitudes were investigated before and after the actuator disk was included. At this speed, the effect of the actuator disk on the scattering coefficients was not found to be of major importance. However, the 2D aerodynamic/3D acoustic incompatibility was found to impact on the scattering coefficients for the rotor alone. Reference 20 found that for either rotor or stator scattering, the maximum pressure transmission coefficient on should be 0dB for a given mode and harmonic scattering into itself. In addition, an upstream going wave being reflected into itself as a downstream going wave should have a scattering coefficient of less than 0dB. The 2D aerodynamics/3D acoustics incompatibility causes the calculation of some of the pressure transmission coefficient magnitudes to be greater than 0dB for a given (m, μ) mode scattering into itself for the same harmonic. For example, a 2BPF $(-9,0)$ mode being transmitted through the rotor at certain speeds has a scattering coefficient of greater than 0dB. Rotor scattering coefficients of greater than 0dB were most common for transmission coefficients, which may be why coupled inlet noise is overpredicted at the high speeds.

The impact of these high coefficients was explored by making a temporary change to the rotor and stator pressure scattering coefficient calculations in SOURCE3D so that for a mode being transmitted into itself, the maximum scattering coefficient would have a magnitude of 0dB. The same was done for upstream going waves being reflected into themselves. The mode phase was not changed. These rotor and stator scattering coefficients were then linked to the associated actuator disk (for turning) using the standard SOURCE3D methods (see Reference 3).

ADP 22" rig predictions resulting from this change are shown in Figure 11. This figure is the same as Figure 8 except for the temporary changes to the rotor and stator pressure scattering coefficient calculations. Comparing these two figures shows that there is little change to aft predictions, and inlet predictions at low speeds. However, for inlet noise at high speeds, both the fully coupled prediction and the rotor/stator coupled inlet 2BPF noise predictions are lower than before the change.

These results are further confirmed by Figure 12 which compares the code rotor/stator coupled predictions with the predictions using this temporary code changes. These results show lower levels of inlet 2BPF at the high speeds with little change in other areas.

Based on these results, we find that rotor scattering transmission coefficient inaccuracies due to 2D aerodynamics and 3D acoustics are an important factor at the high speeds. Calculations also show that this "patch" improves the coupled predictions at the high speeds. In addition, these results indicate that there are other factors impacting on the high speed predictions. The most likely factor is the probable need to further reduce the transmission coefficients for modes transmitted through the rotor into themselves at high speeds. References 20 and 21 discuss the importance of rotor "blockage" on the prediction of inlet noise. In the SOURCE3D calculation (just as in Reference 20), the transmission coefficients (for waves scattered into themselves) are calculated by determining the scattering coefficient and then adding to it the original wave. If these two quantities are of similar magnitude, depending upon the phase, it is possible to completely cancel the wave or double the magnitude. This cancellation effect appears to be underpredicted and is a likely reason for the overprediction of inlet noise at the high speeds.

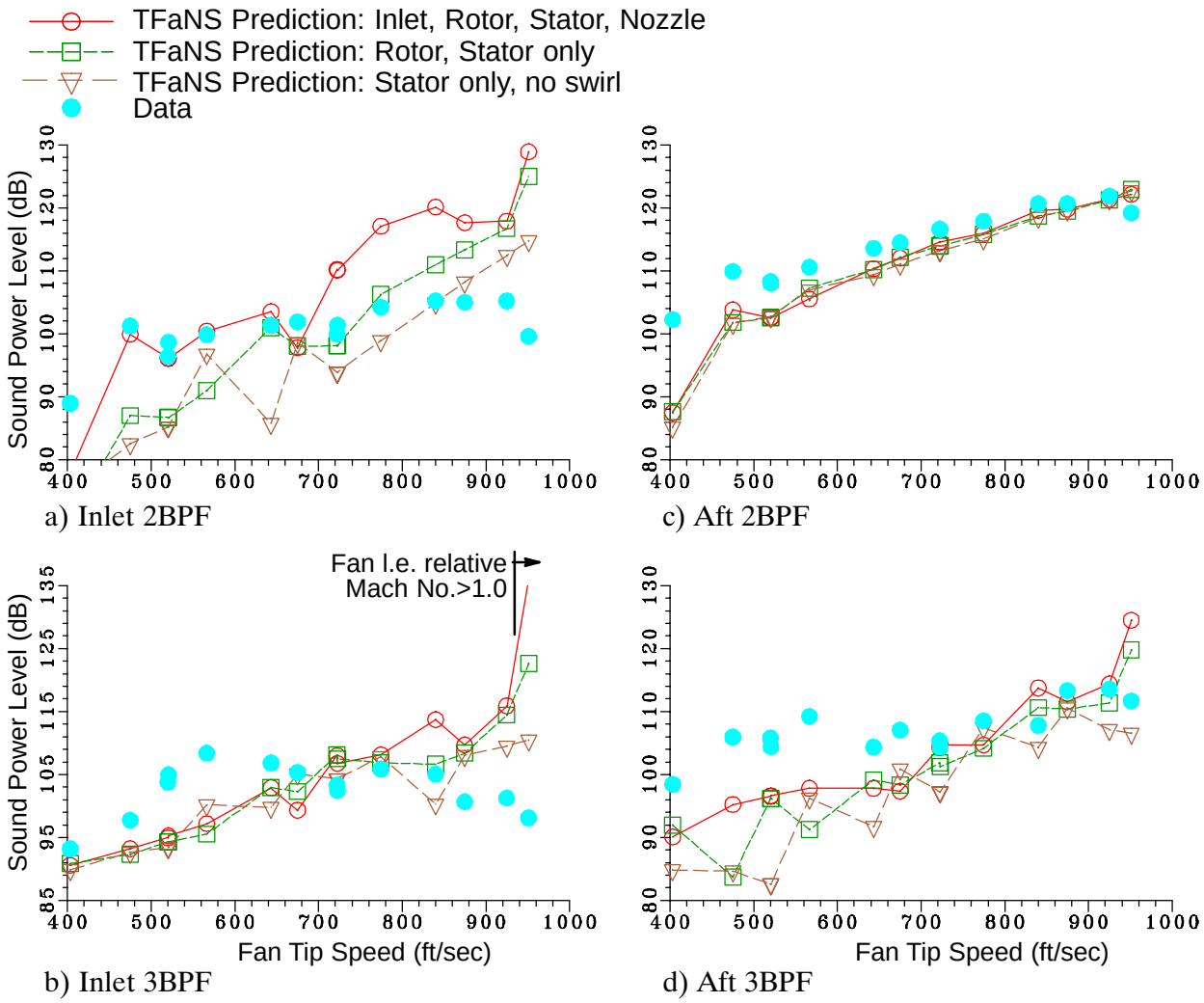

Figure 11: ADP 22" Rig FAN1 Predictions vs. Data with and without inlet and nozzle coupling with certain scattering coefficients set to $\leq$ 0dB for modes scattering into themselves

Other observations for these results include the fact that coupling to the rotor is still important for inlet 2BPF, but overprediction of the data is postponed to a higher speed for the rotor/stator coupled calculation. In addition, at the high speeds, the fully coupled predictions are lower than before, but continue to be higher than the data. These predictions continue to be considerably impacted by aft radiation code results, which are becoming inaccurate in the far−field. Thus, it would be valuable to see what would happen if an improved aft radiation code were used, where the interface between the standard finite elements and the wave envelope elements is better able to handle the size of the noise source.

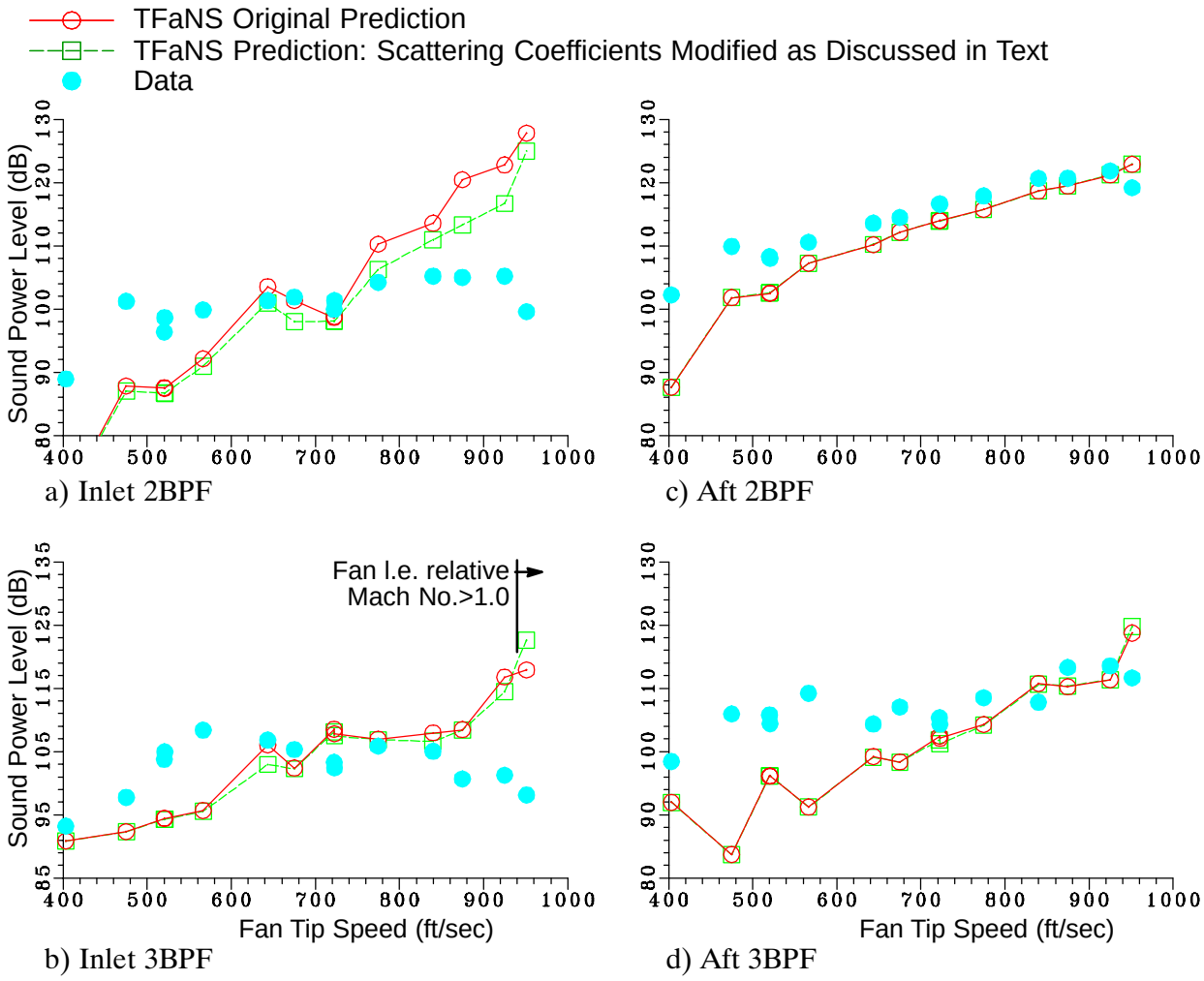

Figure 12: Effect of Scattering Coefficient Modification: ADP 22" Rig FAN1 TFaNS Rotor/Stator Coupled Predictions vs. Data

5. FAR–FIELD SOUND PRESSURE LEVEL TFaNS EVALUATION USING ADP 22” RIG DATA

In this section, TFaNS far−field sound pressure level (SPL) directivity predictions are compared with data for the ADP 22” rig FAN1. Conclusions from the sound power level comparisons from the last section are used to help explain the predictions in the far−field.

Far−field directivity predictions at three speeds are discussed below. As with Section 4.2, three types of predictions are shown: Fully coupled predictions with swirl represent the full capabilities of TFaNS including an inlet, rotor, stator and nozzle with swirl flow and turning. Coupled rotor/stator predictions with swirl but without reflections from the inlet and nozzle give the next level down in predictive capability. Finally, stator only, no swirl with no reflections (coupling) from an inlet, rotor, or nozzle is most like V072 rotor wake/stator interaction code predictions input into the radiation codes. For this last case, the stator upstream interface plane is placed at the same axial location as the rotor leading edge. This makes this configuration consistent with the fully coupled predictions.

Far−field directivities are shown below for the following fan rotational tip speeds: 521 ft/sec, 675 ft/sec, and 775 ft/sec. Corresponding agreement in sound power level is shown in Figure 8 of Section 4.2. This figure shows that at 521 ft/sec tip speed, fully coupled inlet 2BPF sound power level predictions compare well with data whereas rotor/stator coupled and stator only predictions do not compare as well. 3BPF predictions are underpredicted at this speed for all three predictions. At 675 ft/sec tip speed 2BPF power level predictions compare well with data, but 3BPF predictions are still somewhat underpredicted. At 775 ft/sec tip speed, inlet 2BPF power level predictions well overpredict the data. Inlet 3BPF predictions tend to overpredict the data, whereas aft 3BPF predictions tend to predict the data well. The far−field directivity results will now be discussed.

At 521 ft/sec, sound power level results shows coupling has an impact on inlet 2BPF and aft 3BPF power levels. Figure 13 shows 2BPF and 3BPF sound pressure level tone noise directivities at this speed. Figure 13a presents 2BPF predictions which are seen to compare very well with data for the fully coupled results whereas the inlet results for the stator only or rotor/stator coupled predictions are underpredicted consistent with the power level results in Figure 8. At 2BPF, only the $m = -9$ mode is cut on with two contributing radial mode orders.

Predicted far−field directivities are seen to have some “waviness” in the $60 - 110$ degree directivity angle range. This is due to the fact that the inlet and aft complex far−field pressures are being added together for the single propagating $m = -9$ circumferential mode. While this effect is expected when adding inlet and aft noise, it is not known if this effect can be modelled accurately by this system.

In Figure 13b the aft 3BPF fully coupled predictions and rotor/stator coupled predictions compare better with data than does the stator only case consistent with the power level results in Figure 8. Inlet predicted levels are similar although directivities are different. It should be noted that the most important aft 3BPF mode is predicted to be the $(m, \mu) = (9, 2)$ mode which is cut on. The noise from this mode is predicted to come from a forward propagating 2BPF $(m, \mu) = (-9, 2)$ mode which is “mode trapped” in between the rotor and the stator. This is consistent with the power level conclusions in Section 4.2.

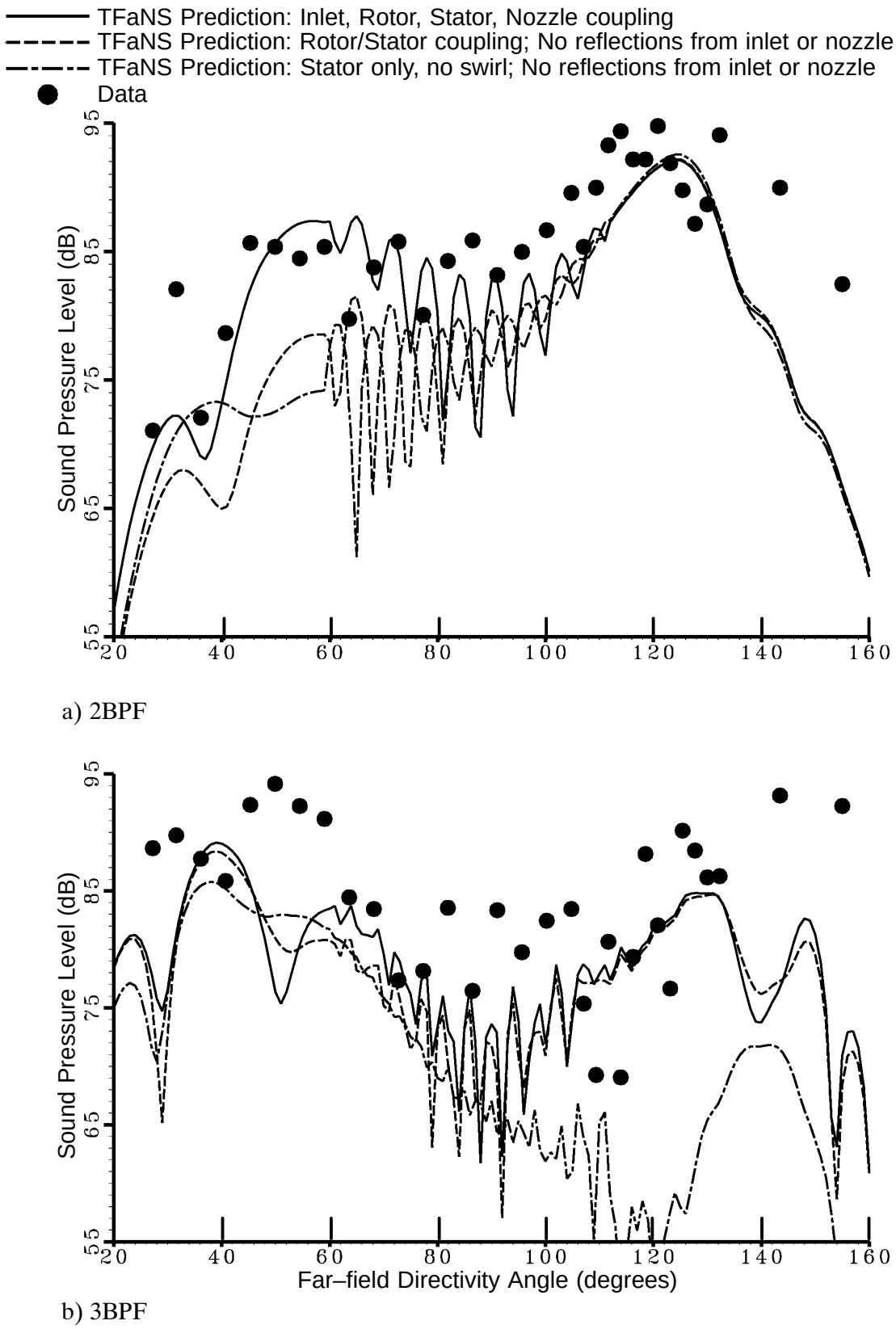

Figure 13: ADP 22" Rig Far−Field Directivities, 521 ft/sec Fan Tip Speed

Figure 14 shows 2BPF and 3BPF sound pressure level tone noise directivities at 675 ft/sec tip speed. Sound power level predictions in Figure 8 show little change in predictions at this speed. Far−field directivities somewhat confirm that, but also show that the small power level differences seen in Figure 8 are reflected in the far−field directivities.

For all three cases, aft 2BPF noise is seen to be reasonably well predicted (just as in the 521 ft/sec tip speed case) with the dominant aft peak occurring where the data says it should. In the inlet, predictions for all three cases compare well with data except forward of a 60 degree directivity angle. In this case, the fully coupled prediction does the best job.

For aft 3BPF, sound power level predictions (Figure 8) show that all aft directivities should be underpredicted, and they are. In the inlet, stator only power level predictions show that the far−field predictions should compare best with data, and they do. This result is consistent with the observation in Section 4.2 that 3BPF noise is underpredicted by this model over a portion of the speed range. As was said earlier, this is possibly due to the wake model.

Figure 15 shows 2BPF and 3BPF sound pressure level tone noise directivities at 775 ft/sec tip speed. Sound power level predictions in this case (Figure 8) show high levels for the fully coupled inlet 2BPF and 3BPF noise. This is reflected in the far−field directivities, especially for inlet 2BPF where predictions are well above the data for the fully coupled predictions. The stator only and rotor/stator coupled predictions compare better for 2BPF out the inlet consistent with the power level results.

Aft 2BPF compares quite well with the data as the sound power level results suggest. Both the aft directivity shape and levels are well predicted which is a promising result for TFaNS and the aft radiation code.

Far−field directivities at 3BPF do not match in level or shape in the inlet even though predicted sound power levels only slightly overpredict the data. This is probably more a function of the middle angle range importance in the power level calculations where far−field directivities compare better in level but not in shape. Aft 3BPF directivities for the rotor/stator coupled and fully coupled predictions show similarities to the data whereas the stator only, no swirl calculation underpredicts the data.

In the middle angle range, Figure 15 shows irregular “waviness” for both harmonics. These patterns are indications that the aft radiation code far−field directivities are starting to break apart. This may impact on the aft radiation code reflection coefficients as discussed in Section 4.4.

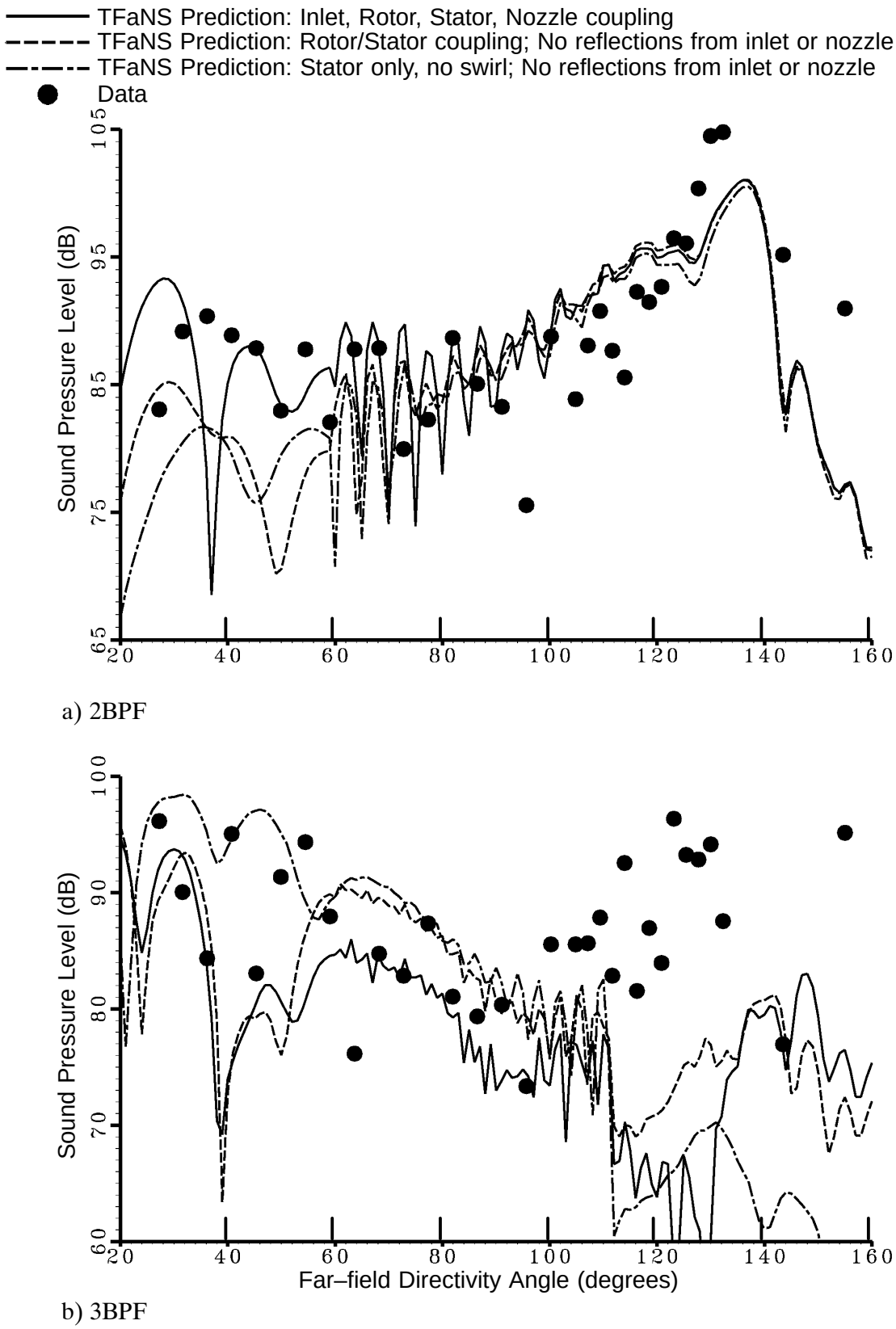

Figure 14: ADP 22" Rig Far−Field Directivities, 675 ft/sec Fan Tip Speed

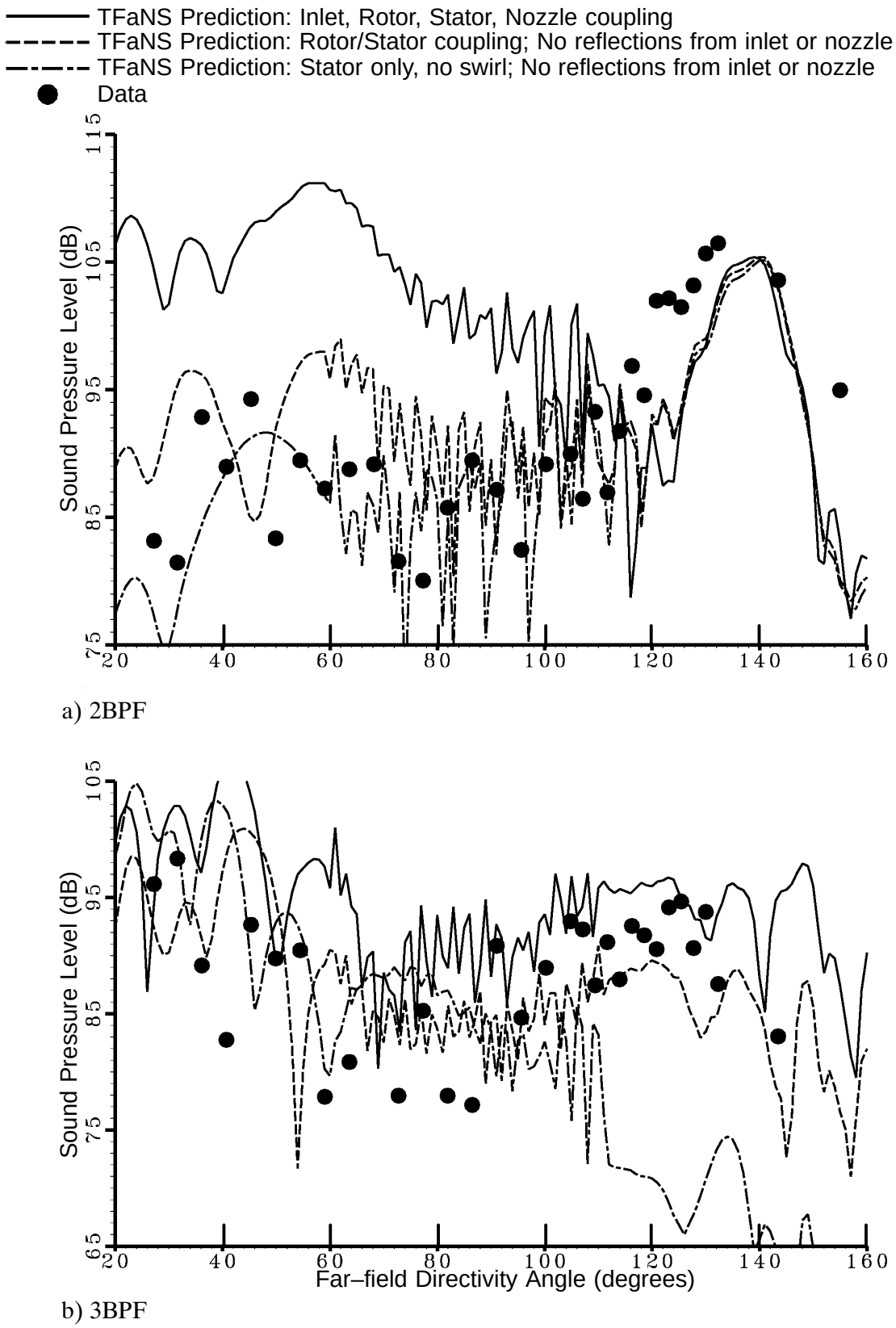

Figure 15: ADP 22" Rig Far−Field Directivities, 775 ft/sec Fan Tip Speed

6. CONCLUSIONS

A coupled fan noise design/prediction system, TFaNS, has been developed and evaluated with full scale engine and ADP 22" fan rig data. This system is capable of coupling an inlet, rotor, stator, and nozzle to calculate far−field directivities and power levels. The present system is limited to subsonic rotors.

The following conclusions have been made from this evaluation:

- Overall, TFaNS is capable of predicting sound power levels for a rotor coupled to a stator (without inlet or nozzle coupling):
  - For aft noise, predictions compare better with data than uncoupled stator only predictions for subsonic fan leading edge relative Mach numbers.
  - For inlet noise, results compare better with data than uncoupled stator only predictions for tip speeds below about 700 − 750 ft/sec for the fan rig and below about 1000 ft/sec for the full scale engine.
  - The system overpredicts inlet noise above fan tip speeds of about 700 −750 ft/sec for the fan rig and above about 1000 ft/sec for the full scale engine. This appears to be due in part to the formulation in the SOURCE3D rotor wake/stator interaction code which couples 2D aerodynamics and 3D acoustics. The rotor unsteady pressure distribution calculation alone (which has trouble at high Mach numbers and high frequencies) may also contribute, especially for the full scale engine inlet noise predictions where the rotor leading edge Mach number becomes supersonic above 1000 ft/sec tip speed.
- An experiment making simple modifications to specific transmission and reflection coefficients shows the impact of the mixing 2D aerodynamics and 3D acoustics for coupling. Predictions during this experiment using the ADP 22" rig configuration improved inlet propagating power levels above 700 − 750 ft/sec fan tip speed. Results show that rotor transmission coefficients may be too high, especially for modes at a given harmonic being scattered into themselves. These high transmission coefficients may be the most important reason for inlet power level overprediction at high speeds in the ADP 22" rig.
- TFaNS rotor/stator coupling predicts general trends seen in the full scale engine data when the rotor is subsonic. The significant rise in aft 3BPF seen in Reference 10 due to a "trapped" BPF mode was well modelled for the 1.9 vane/blade ratio configuration. The 2.2 vane/blade ratio configuration did not duplicate the entire rise shown by the data, but showed a significant improvement over the stator only, no swirl (V072 rotor wake/stator interaction type) predictions.
- "Fully Coupled" (i.e. inlet/rotor/stator/nozzle coupled) TFaNS predicted sound power levels for the ADP 22" rig FAN1 tend to do the best job of predicting inlet and aft tone sound power levels except for inlet noise above tip speeds of about 700 − 750 ft/sec. In this latter case, including an inlet and nozzle further exaggerates the overpredicted results. This appears to be primarily due to high nozzle reflection coefficients and high rotor transmission coefficients. Both the nozzle and the rotor calculations appear to be having some trouble predicting noise at the higher speeds.
- For supersonic fan leading edge relative Mach numbers, rotor/stator coupling overpredicts absolute inlet tone noise levels for the full scale engine. This may be due to the fact that there are shocks on the rotor which should block more of the inlet noise than is being predicted. Also, at these speeds, the rotor cascade pressure distribution calculation begins to have difficulties because of the subsonic nature of the model, and the small upstream going pressure wavelengths which exist at these high speeds.
- Far field directivity predictions for the ADP 22" rig FAN1 rig appear to compare well with data when sound power level predictions compare well, and do not compare well with data when sound

power level predictions do not compare well. Higher frequency predictions at 3BPF do not compare with data as well as 2BPF predictions.

- Nozzle predictions show some problems at higher speeds and reduced frequencies due to the size of the source (which includes the shear layer). In the present code the source size can cause waves to reflect off the boundary between the standard finite elements and the wave envelope elements.
- ADP 22" rig FAN1 levels for inlet and aft 3BPF at low speeds may be underpredicted by the system because of the wake model in SOURCE3D. The wake model uses high speed fan rig data at or near the design speed of the rig. Thus off design (low speed) wake predictions may be sometimes incorrectly predicted. Some initial work with measured wakes from the ADP 22" rig show this to be a reasonable possibility. Work with the measured wakes are anticipated to be presented in a future report under a later contract.

7. RECOMMENDATIONS

7.1 SOURCE3D IMPROVEMENTS

- Work should be done to more effectively deal with the 2D aerodynamic/3D acoustic issue to make TFaNS a useful tool for inlet noise prediction. Particular attention should be paid to the rotor transmission coefficients for modes being scattered into themselves for a given harmonic.
- A high frequency cascade pressure distribution calculation model should be incorporated in the code for the high speed, high frequency operation.
- A method should be developed to calculate the unsteady pressure distribution on a supersonic or transonic rotor. This method should then be coupled to a noise model in a subsonic duct flow. The ability to handle shocks on the rotor is also desirable.
- The definitions of input parameters to the SOURCE3D rotor wake/stator interaction code need to be further investigated including the effects of rotor and stator stagger angle definitions, the solid body swirl assumption and steady flow Mach number definitions.

7.2 RADIATION CODE IMPROVEMENTS

Work to make the aft radiation code more accurate at higher frequencies. Possible methods for accomplishing this include:

- Eliminating the baffles in both the inlet and aft radiation codes.
- Work to improve the wave envelope region and its interface with the standard finite element regions in the aft radiation code.

Professor W. Eversman of the University of Missouri − Rolla is presently working on these issues.

7.3 OTHER IMPROVEMENTS

- Improve the wake modelling component of the design system. This should include both the improvement of semi−empirical wake models along with the development of accurate methods for predicting wakes from computational fluid dynamic methods.
- Move on to higher level noise design methodology. This could take the form of:
  - Implement lifting surface theory type unsteady pressure response functions in SOURCE3D. This would eliminate the approximations associated with 2D aerodynamics and 3D acoustics.
  - Replace SOURCE3D with a linearized Euler code with true non−reflecting boundary conditions. This would eliminate the approximations associated with 2D aerodynamics and 3D acoustics as well as eliminating issues associated with calculating unsteady pressures on cascades of flat plates.

8. REFERENCES

1 Hanson, D. B., "Mode Trapping in Coupled 2D Cascades − Acoustic and Aerodynamic Results," AIAA−93−4417, October 1993.

2 Topol, D. A., "Tone Fan Noise Design/Prediction System, Volume I: System Description, CUP3D Technical Documentation and Manual for Code Developers," NASA−CR−XXXXXX, May 22, 1998.

3 Meyer, H. D., "Source Methodology for Turbofan Noise Prediction (SOURCE3D Technical Documentation)," NASA−CR−XXXX, December 1997.

4 Roy, I. D., and Eversman, W., and Meyer, H. D.,"Improved Finite Element Modeling of the Turbofan Engine Inlet Radiation Problem," Informal Report to NASA Lewis under NASA Contract NAS3−25952 (Task 10), April 1993.

5 Roy, I. D., and Eversman, W., "Development of the Turbofan Acoustic Radiation Code: Code Improvements, Acoustic Treatment, and Aft Radiation Including Shear Layer Effects," Informal Report to NASA Lewis under NASA Contract NAS3−26618 (Task 4), May 1994.

6 Eversman, W., and Okunbor, D., "Development of the Inlet and Aft Fan Duct Acoustic Radiation Codes," Informal Report to NASA Lewis under NASA Grant NASA NAG3 1678, April 1996.

7 Eversman, W., and Okunbor, D., "An Improved Finite Element Formulation for Aft Fan Duct Acoustic Radiation," Informal Report to NASA Lewis under NASA Grant NASA NAG3 1678, June 1997.

8 Topol, D. A., "Technical Documentation for the AWAKEN Wake/Turbulence Postprocessor," to be Published under the Advanced Subsonic Technology Contract (Task 13), NAS3−27727 in late 1999.

9 Topol, D. A and Eversman, W., "Tone Fan Noise Design/Prediction System, Volume II: User Manual, TFaNS Vers. 1.4," NASA−CR−XXXXXX, July 14, 1998.

10 Topol, D. A., Holhubner, S. C., and Mathews, D. C., "A Reflection Mechanism for Aft Fan Tone Noise From Turbofan Engines," AIAA−87−2699, October 1987.

11 Hanson, D. B., "Unsteady Coupled Cascade Theory Applied to the Rotor/Stator Interaction Noise Problem," DGLR/AIAA−92−02−084, May 1992.

12 Hanson, D. B., "Acoustic Reflection and Transmission of Rotors and Stators, Including Mode and Frequency Scattering," AIAA−97−1610, May 1997.

13 Smith, S. N., Discrete Frequency Sound Generation in Axial Flow Turbomachines," R&M No. 3079, 1973.

14 Topol, D. A., and Mathews, D. C., "BBN/PW V072 Rotor Wake/Stator Interaction Code − Technical Documentation and User's Manual," NASA Contract NAS3−25952 (Task 10), April 1993.

15 Topol, D. A., "Rotor Wake/Stator Interaction Noise − Predictions Versus Data," , Journal of Aircraft, Vol. 30, No. 5, p.p. 728−735, September/October 1993.

16 Meyer, H. D. and Envia, E., "Aeroacoustic Analysis of Turbofan Noise Generation," NASA CR−4715, March 1996.

17 Majjigi, R. K., and Gliebe, P. R., "Development of a Rotor Wake/Vortex Model," NASA−CR−174849, June 1984.

18 Topol, D. A., and Philbrick, D. A., "Fan Noise Prediction System Development: Wake Model Improvements and Code Evaluation," Informal Report under NASA Contract NAS3−25952 (Task 10), April 1993.

19 Eversman, W., Private Communication with D. A. Topol.

20 Hanson, D. B., "Acoustic Reflection and Transmission of Rotors and Stators Including Mode and Frequency Scattering," AIAA/CEAS 97−1610, May 1997.

21 Philpot, M. G., "The Role of Rotor Blade Blockage in the Propagation of Fan Noise Interaction Tones," AIAA−75−447, March 1975.

APPENDIX I:
DEVELOPMENT AND EVALUATION OF SOURCE3D CHORDWISE INTEGRATION STATION CRITERIA

Internal Correspondence

UNITED TECHNOLOGIES PRATT & WHITNEY

To: D. A. Topol

cc: D. B. Hanson
W. B. Wagner

From: M. L. Abelson **M/S:** 161–22 **Ext:** 5–8134

Subject: Development and Evaluation of SOURCE3D Chordwise Integration Station Criteria

Date: December 20, 1995

REFERENCES:

1. Smith, S. N., Discrete Frequency Sound Generation in Axial Flow Turbomachines," R&M No. 3079, 1973.

2. Ventres, C. S., Theobald, M. A., and Mark, W. D., "Turbofan Noise Generation, Volume 1: Analysis," NASA CR−167951, July 1982

3. Topol, D. A. and Mathews, D. C., "BBN/PW V072 Rotor Wake/Stator Interaction Code − Technical Documentation and User's Manual," NASA Contract NAS3−25952 (Task 10), April 1993.

4. Topol, D. A., "TFaNS Theoretical Fan Noise Design/Prediction System; System Description and Manual for Users and Code Developers (PRELIMINARY)," NAS3−26618 (Task 4), August 1995

I.1 SUMMARY:

An evaluation was done to formulate chordwise integration station criteria for the newly developed Rotor Wake/Stator Interaction Code, SOURCE3D. Using a criterion that exists in SOURCE3D's predecessor, V072, as a starting point, we investigated several possible criteria using the code written by Smith, and then SOURCE3D itself. SOURCE3D contains an unsteady pressure calculation which requires the number of integration stations, or panels, in the chordwise direction to be specified. Previously, the user had to decide for himself how many panels he wanted to use and this number would be used for the rotor and the stator at every radius. With the development of the new criteria, the code will determine the appropriate number of panels for each radius on the rotor and stator.

There were several reasons for wanting to develop these criteria. If the number of panels selected is too high, in relation to the number actually needed for convergence, the pressure calculation starts to become unstable. If this problem is avoided, then the confidence in the accuracy of the prediction can be higher. We also hoped to save time in the actual running of the code. The number of panels directly affects the amount of CPU time required, so minimizing the number of panels will minimize CPU time.

We ran SOURCE3D for several test cases and compared the new predictions with old results. The old results were previously considered to be the "best", based on experience. Our observations to this time are discussed below and indicate that the criteria that were developed are adequate.

I.2 DEVELOPMENT OF THE INTEGRATION STATION CRITERIA

We used the code written by Smith (Ref. 1.) because it was a similar formulation of the unsteady pressure distribution calculation that is found in the V072 Rotor Wake/ Stator Interaction Code (Ref. 2.), which SOURCE3D is based on. The calculation contained in the Smith code is a lot easier to isolate and work with than the one in V072. A driver was created which allowed us to run a range of panels to find the minimum number of panels required to get the pressure calculation to converge. It also permitted variation of the input circumferential mode number and the number of harmonics that were run for each test case. Unsteady pressure and far field pressure distributions were also printed for plotting. The geometries for the stator and the rotor can be seen in Figure 1 and Figure 2 respectively.

It was believed that the number of panels would depend on the wavelength of either the vorticity, upstream pressure, or downstream pressure waves since these are the only waves creating the unsteady pressures. V072 already contained a criterion (Ref. 3.) which determined the number of panels, N_{chord}, for the stator based on the vorticity wave number, K_3. Assuming 2π points per wavelength:

$$K_3 = \frac{\omega b}{u} = \frac{nBM_\theta b}{Mr} \tag{1}$$

$$N_{points} = 2\pi \tag{2}$$

$$N_{chord} = K_I \left[\frac{N_{points}}{2\pi} \right] \tag{3}$$

The pressure calculation requires the number of panels to be even, so the criterion states that the number of panels is based on the value of N_{chord} rounded up to the next even integer.

I.2.1 The Stator

The stator geometry is represented in Figure 1. Wakes from the turning blades hit the stators and cause unsteady pressures to form on the cascade. A mode, m, enters the stator for a given rotor harmonic, n, and "scatters" into infinite outgoing modes by varying k. Blade passing frequency, BPF, is described by the number, n, of the rotor harmonic. By using the input parameters to the driver we could calculate equations (4) and (5) for several harmonics.

$$K_{1,2} = \left(\gamma_{1,2} \cos\theta_D - m \sin\theta_D\right)\frac{b}{r} \tag{4}$$

$$K_3 = \frac{nBM_\theta b}{Mr} \tag{5}$$

K_3 is the vorticity wave reduced frequency, K_1 and K_2 are the upstream and downstream pressure wave reduced frequencies respectively, where

$$\gamma_{1,2} = \frac{M_{axial}\left(nBM_\theta - mM_{swirl}\right) \pm K_{mn}}{1 - M_{axial}^2} \tag{6}$$

$$K_{mn} = \sqrt{\left(nBM_\theta - mM_{swirl}\right)^2 - \left(1 - M_{axial}^2\right)m^2} \tag{7}$$

$$m = nB - kV \tag{8}$$

The number of points required, N_{chord}, is found by equation (3) where I = 1, 2 & 3 from above. Currently we are using 2π points per wavelength, so N_{chord} is simply the value of the reduced frequency of the wave in question. As in the V072 criterion, the value of N_{chord} is rounded up to the next even integer.

The baseline case was the ADP 22" Rig . Different test cases were created by varying input parameters such as Mach number, radius, and number of blades. After running the modified version of the Smith code we were able to produce plots like the one in Figure 3, which shows the far field pressure as a function of the number of panels for the upstream going wave on the stator. The test case that produced Figure 3 was run with 18 blades and 45 vanes at a radius of 11.00 inches. As you can see from this plot, the smallest number of panels needed for the calculation to converge is 8, since all three input waves have converged by this number. Convergence is defined as the point where the far field pressure distribution oscillations become within ± 1 dB of the final value. In order to determine the number of panels necessary for this harmonic, at this radius, plots like Figure 3 were created for all three output waves (vorticity, upstream pressure, downstream pressure). It was seen that within each harmonic, n, that the calculation converged at the same time regardless of the value of k. The output from equations (4),(5), (7), and (8) for the sample case of Figure 3 can be found in Table I.

TABLE I
SAMPLE OUTPUT FOR STATOR (VORTICITY WAVELENGTH IS SHORTEST)

Mode	K_{mn}	K_1	K_2	K_3	cuton/cutoff
54	42.077	3.25	3.25	7.30	cutoff
9	38.296	3.07	2.05	7.30	cuton
−36	36.622	5.09	0.17	7.30	cuton
−81	46.333	5.68	5.68	7.30	cutoff
−126	94.853	9.37	9.37	7.30	cutoff

The first criterion that we wanted to check was the vorticity wave criterion which already existed in V072. In the above case, the reduced frequency of the vorticity wave, K_3, is 7.30, and when this is rounded up to the next even integer, you get the value of 8 panels which is what we saw in Figure 3.

Figure 4 shows the results of this criterion on the stator. The number of panels that were observed from the far field pressure plots, such as Figure 3, are on the y axis and the number of panels predicted by the criterion are on the x axis. The ideal line represents the observed value being equal to the predicted value (i.e., x=y). The circles represent the vorticity prediction for cases when the vorticity wave was shortest and the squares represent the vorticity prediction for cases when the pressure wave was shortest. It can be seen that when the pressure wave is shortest that the criterion underpredicts slightly and when the vorticity wave is shortest, the prediction falls on the ideal line.

The second criterion was the pressure wave criterion. Experience found that the downstream pressure wave, K_2, never dominated the problem. Thus, all of the discussions below concentrate on the upstream propagating pressure wavelengths. In order to choose the number of panels when the upstream pressure was the shortest wave, we chose the value of K_1 for the cuton mode with the shortest wavelength (highest wave number, K_1); this is known as the "last cuton mode" criterion because the highest cuton value of K_1 always occurs at the mode just before cutoff. In Table I, this would be the m=−36 mode and it would have picked 6 Panels (5.09 rounded up to the next even integer) which is too low. The pressure wave criterion was modified after an interesting behavior of the problem was noticed. The number of panels necessary seemed to be linked in some way to the maximum value of K_{mn} for the cuton modes. For example, from Table I, we would pick the m=9 mode as the maximum value of Kmn for the cuton modes. Thus, the "maximum K_{mn} criterion" would predict 4 Panels.

However, since the pressure wave is not the shortest wave in this sample case, this only represents the method that was used and is not an actual prediction. Figure 5a and Figure 5b show the two pressure criteria results on the stator. In Figure 5a you can see that the last cuton mode criterion overpredicts when the pressure wave is shortest and underpredicts when the vorticity wave is shortest. In Figure 5b you can see the same results as in Figure 5a, however, the overprediction when the pressure wave is shortest is far less, making the "max K_{mn}" criterion the better choice.

As a final criterion it was decided to use both the vorticity wave and the pressure wave to determine the number of panels. The vorticity criterion would be used when the vorticity wave had the shortest wavelength of the cuton modes, as in Table I, and the "max K_{mn} criterion" would be used when the pressure wave had the shortest wavelength of all the cuton modes.

I.2.2 The Rotor

The rotor geometry is represented in Figure 2. Essentially, the problem is now treated as if the blades were held stationary and the vanes were turning in the direction of M_θ. Waves are sent from the vanes to the blades causing unsteady pressure distributions on the blades. A mode, m, enters the rotor for a given stator harmonic, k, and "scatters" into infinite outgoing modes by varying n. Vane passing frequency, VPF, is described by the number, k, of the stator harmonic. For the problem of the rotor, the equations used in the stator criterion change slightly and become:

$$K_{1,2} = \left(\gamma_{1,2}\cos\alpha_r - m\sin\alpha_r\right)\frac{b}{r} \tag{9}$$

$$K_3 = \frac{kVM_\theta b}{Mr} \tag{10}$$

$$\gamma_{1,2} = \frac{M_{axial}\left(kVM_\theta - mM_{swirl}\right) \pm K_{mn}}{1 - M_{axial}^2} \tag{11}$$

$$K_{mn} = \sqrt{\left(kVM_\theta - mM_{swirl}\right)^2 - \left(1 - M_{axial}^2\right)m^2} \tag{12}$$

and the mode now becomes:

$$m = -nB + kV \tag{13}$$

Figure 6 represents a far field pressure distribution for an upstream going wave on the rotor for a test case with 18 blades and 24 vanes at a radius of 9.67 inches. From this plot it can be seen that the calculation converges at about 54 panels since the three input waves have converged. We found that for our test cases that the vorticity wave was rarely the shortest wave on the rotor and, as can be seen in Figure 7, the vorticity criterion severely underpredicted the number of panels necessary. This is due to the high Mach numbers that exist on the rotor. At lower Mach numbers, the vorticity wave would be more likely to dominate. As with the stator, the downstream pressure wave never had the shortest wavelength. That left us with only the upstream pressure wave to determine the number of panels necessary. The output from equations (9), (10), (12) and (13) for the test case of Figure 6 can be seen in Table II.

TABLE II
SAMPLE OUTPUT FOR ROTOR (PRESSURE WAVELENGTH IS SHORTEST)

Mode	K_{mn}	K_1	K_2	K_3	cuton/cutoff
30	22.277	10.26	10.26	14.45	cutoff
12	21.962	8.22	6.68	14.45	cuton
−6	36.072	20.73	3.75	14.45	cuton
−24	44.275	31.23	1.17	14.45	cuton
−42	49.594	40.75	7.08	14.45	cuton
−60	52.906	49.59	13.67	14.45	cuton
−78	54.578	57.87	20.81	14.45	cuton
−96	54.760	65.64	28.47	14.45	cuton
−114	53.468	72.92	36.62	14.45	cuton
−132	50.589	79.66	45.31	14.45	cuton
−150	45.824	85.75	54.64	14.45	cuton
−168	38.480	90.98	64.85	14.45	cuton
−186	26.491	94.62	76.63	14.45	cuton
−204	15.393	93.49	93.49	14.45	cutoff

From Table II, the "last cuton mode" criterion would pick the $m=-186$ mode as the cuton mode with the highest value of K_1, and predict 96 panels. The "max K_{mn}" criterion would pick the $m=-96$ mode as the cuton mode with the highest value of K_{mn}, and would predict 66 panels. Since the observed number of panels was 54, the max K_{mn} criteria seems to work better. Our results for these two criteria can be seen in Figure 8a and Figure 8b. Figure 8 shows that on the rotor, where the pressure wave is shortest, the best prediction method is the "max K_{mn}" criterion. It usually overpredicts, but it overpredicts noticeably less then the "last cuton mode" criterion.

I.3 PROCEDURE FOR TESTING CRITERIA IN SOURCE3D

V072 previously contained a criterion (Ref. 3.) which would determine the number of panels on the stator. During our evaluation, we determined that the "max K_{mn}" criterion is an improvement to this criterion for situations in which the pressure wave has the shortest wavelength. However, it was decided only to include the original criterion in SOURCE3D at this time. This was do to the fact that the stator calculation is relatively stable and will not be affected greatly by small errors in the predicted number of panels.

A new routine was added to SOURCE3D which determines the number of panels required for each radius on the rotor for each harmonic. When the vorticity wave has the shortest wavelength, usually at lower speeds, then the vorticity wave in equation (10) is used. When the pressure wave has the shortest wavelength, then the "max K_{mn}" criterion is used. In order to be able to find the maximum value of K_{mn} within the code, the following method was developed. The circumferential mode number, N_{max}, where the maximum value of K_{mn} exists was found by taking the derivative of equation (12) with respect to n and solving for n when the derivative was set to zero. A constant of 0.5 was added at the end so that when the integer of the result was taken, it would round off correctly and the result is shown in equation (14). The mode where K_{mn} is a maximum can be found for each harmonic of k from equation (15). This mode number is then used in equation (12) to find the maximum value of K_{mn}. This value is then used in equation (11) and then in equation (9) to determine the value of K_1.

$$N_{\max} = integer\left[\frac{kV}{B}\left(1 + \frac{M_\theta M_{rr}\sin\alpha_r}{1 - M_{rr}^2}\right) + 0.5\right] \tag{14}$$

$$m = -N_{\max}B + kV \tag{15}$$

The V072 pressure calculation, which is what SOURCE3D is based on, is a little more unstable on the rotor than the Smith code which makes it very important not to underpredict or over predict the actual number of panels necessary by too many panels. Figure 9 shows the unsteady pressure distributions, from SOURCE3D, for several different number of panels. These distributions were produced from a test run of the ADP 17" rig with 16 blades and 22 vanes at the rotor tip and for an N_{1C} of 9600 rpm. Figure 9a shows the unsteady pressure distribution with 18 panels (selected by the criterion) and Figure 9b shows the calculation done with 32 panels (previously chosen to be the best number of panels). These two plots are very similar, however, Figure 9c shows what happens to the calculation when 60 panels are used, which grossly exceeds the actual amount necessary. The calculation starts to oscillate at the leading and trailing edges.

I.4 EVALUATION OF CRITERIA IN SOURCE3D

In order to evaluate the performance of the new version of SOURCE3D, we compared its new predictions to those that were previously considered to be the best. The test case was run for the ADP 17" Rig with 16 Blades and 22 Vanes. This test case covered a range of speeds and actual test data was available to compare the predictions to. We evaluated four different setups of this test case and they can be seen in Table III. Our baseline case was run with 32 panels on the stator and the rotor for all radii, which is how the previous version was run. The code was also left to determine the number of panels on the stator and we chose 32 panels for the rotor. This would show how well the stator criterion was working. We then used the stator criterion again and picked 60 panels for the rotor. This was done to check out the results when we reached the maximum number of panels allowed by the code. We also allowed SOURCE3D to pick the number of panels on the rotor and the stator based on the criteria.

TABLE III
RUN CONFIGURATIONS FOR SOURCE3D EVALUATION

Number of Panels on the Stator	Number of Panels on the Rotor
Chosen to be 32	Chosen to be 32
Chosen by Criterion	Chosen to be 32
Chosen by Criterion	Chosen to be 60
Chosen by Criterion	Chosen by criterion

In order to compare the results for SOURCE3D we ran SOURCE3D version 1.1 and CUP3D version 2.0 as part of TFaNS version 1.1 (Ref 4.). SOURCE3D produces acoustic properties files (Ref 4.) for the rotor and stator which contain scattering matrices composed of mode reflection and transmission coefficients. CUP3D (Ref 4.) is a code that couples the acoustic properties files and produces a far field power level prediction. Figure 10 shows the power level predictions produced by TFaNS. These graphs show that there were very slight differences between these test cases. The only major difference was at Inlet BPF at a tip speed of 722 Ft/s (N_{1C} = 9600 rpm). At this speed, the case of setting 60 panels for the rotor predicted levels 6 dB higher than the other three cases. The same case had about a 1.5 dB higher prediction at Inlet 2BPF for the same speed. The case of 60 panels and the case of the criteria predicted about 2 dB higher at the highest speed of Inlet BPF and Inlet 3BPF. There were only minor differences of less than 1 dB over the rest of the data.

Another area that was looked into was the possibility of increasing the maximum number of panels allowed in the code (currently 60) to see if that would change results. If the results were not changed then it might allow the user to run more than 3 harmonics, which is the suggested limit of the code at the present time. We allowed the code to use the criteria and varied the maximum number of panels allowed between 60, 80, and 100. Figure 11 shows part of the results showing that the power level predictions were identical at all three different levels. This was also the case for all other inlet and aft harmonics through 3BPF.

We also looked at the unsteady pressure distributions on the cascade and found that they were beginning to show signs of instability as 60 panels was approached. We attempted to correct this problem by changing the convergence criterion in the kernel function of the pressure calculation. We decided to vary the error term which controls convergence from a value of 10^{-4} to a value of 10^{-12}. Results for the first harmonic are shown in Figure 12, where we noticed no changes in the final power levels produced by TFaNS. Other harmonics produced similar results.

One final result was that the amount of time that it takes SOURCE3D to run when it is using the criteria is less than the time is takes to run when the user chooses the number of panels necessary. SOURCE3D ran approximately 1 hour and 10 minutes faster for the 12 speed run that produced Figure 10, when the criteria were used, over when 32 panels were used for the rotor and stator. These times are for a Sun SPARC station 20.

I.5 CONCLUSIONS & RECOMMENDATIONS

In the past, SOURCE3D needed to be run for a range of panels to decide what the appropriate number of panels was for a single test case. Your only option was to pick a certain number of panels that would be applied to the stator and the rotor (two totally different environments) for every radius and every harmonic. Now with the creation of the rotor criterion, it is possible to run SOURCE3D only once and the code will pick the correct number of panels for the stator and the rotor at each radius for each harmonic.

Based on the results we obtained in this study, there is a good deal of confidence in the criteria developed. More testing needs to be done to get a feel of how the results behave for cases other than the one we tested. In addition there are several things that would make sense to do in the future.

1. The stator criteria should be changed so that it includes the "maximum K_{mn}" criterion.

2. An investigation of why the "max K_{mn}" criterion works might lead to a better criterion which would predict a better number of panels.

3. Run the Smith code for a case that causes the pressure distribution in V072 to give unstable results and see how the Smith code behaves.

4. Run the 22" rig configuration and see if the predictions are acceptable.

5. Try running SOURCE3D setting the number of panels on the rotor to 80 and 100 and see how the prediction changes. It may be possible to increase the maximum number of panels.

6. Try running SOURCE3D up to 4BPF and 5BPF rather than 3BPF which is what the assumed limits of the code are at this time. In order to do this, the maximum number of panels would have to be raised.

7. Modify Smith/V072 to reduce instability at high frequencies

LIST OF SYMBOLS FOR APPENDIX I

PARAMETERS

α_r = *rotor stagger angle measured relative to the axial direction*
b = *chord of cascade for which the pressure distribution is being calculated*
B = *number of blades*
BPF = *blade passing frequency*
γ_1 = *upstream pressure wave axial wavenumber*
γ_2 = *downstream pressure wave axial wavenumber*
k = *an integer,* $-\infty < k < +\infty$, *when* $m = nB - kV$ *(stator); harmonic of VPF when* $m = -nB + kV$ *(rotor)*
K_{mn} = *defined in equation. (7) for stator and equation. (12) for rotor*
K_1 = *upstream going pressure wave reduced frequency in chordwise direction*
K_2 = *downstream going pressure wave reduced frequency in chordwise direction*
K_3 = *vorticity wave reduced frequency*
m = *circumferential mode order where: m is positive in the direction of rotor rotation for stator calculation; m is positive opposite the direction of rotor rotation for rotor calculation*
M_{axial} = *axial Mach number*
M_{rr} = *Mach number relative to the rotor*
M_{swirl} = *swirl Mach number*
M_θ = *rotational Mach number*
n = *harmonic of BPF when* $m = nB - kV$ *(stator); an integer,* $-\infty < k < +\infty$, *when* $m = -nB + kV$ *(rotor)*
N_{1C} = *corrected rotational speed in rpm*
N_{chord} = *number of chordwise integration stations chosen by the criteria*
N_{max} = *an integer,* $-\infty < k < +\infty$, when $m = -N_{max}B + kV$ *where* K_{mn} *is maximum*
N_{points} = *number of integration stations per wavelength*
θ_D = *stator stagger angle measured relative to the axial direction*
r = *radius*
ϱ = *mean density*
u = *mean velocity*
V = *number of vanes*
VPF = *vane passing frequency*
ω = *rotational frequency in rad/s*

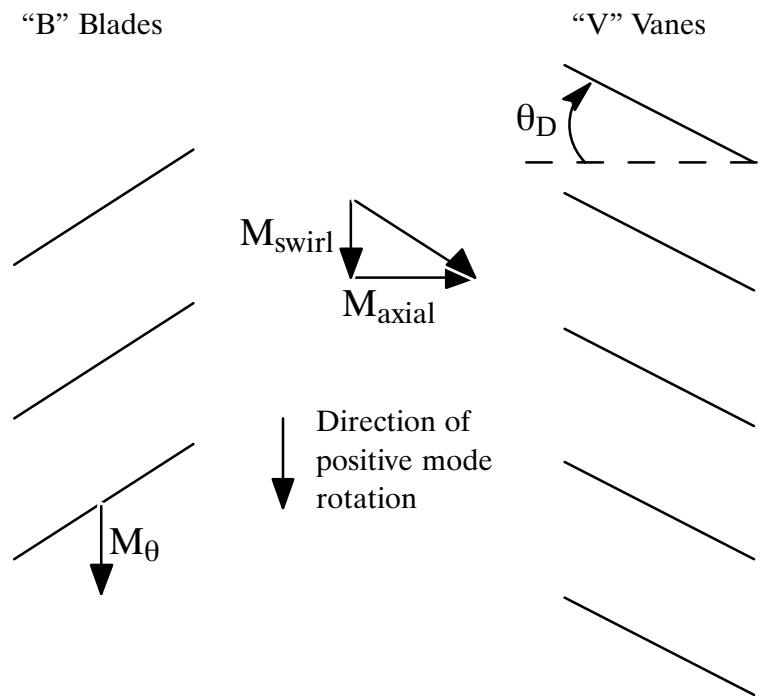

Figure 1 Geometry for the Stator

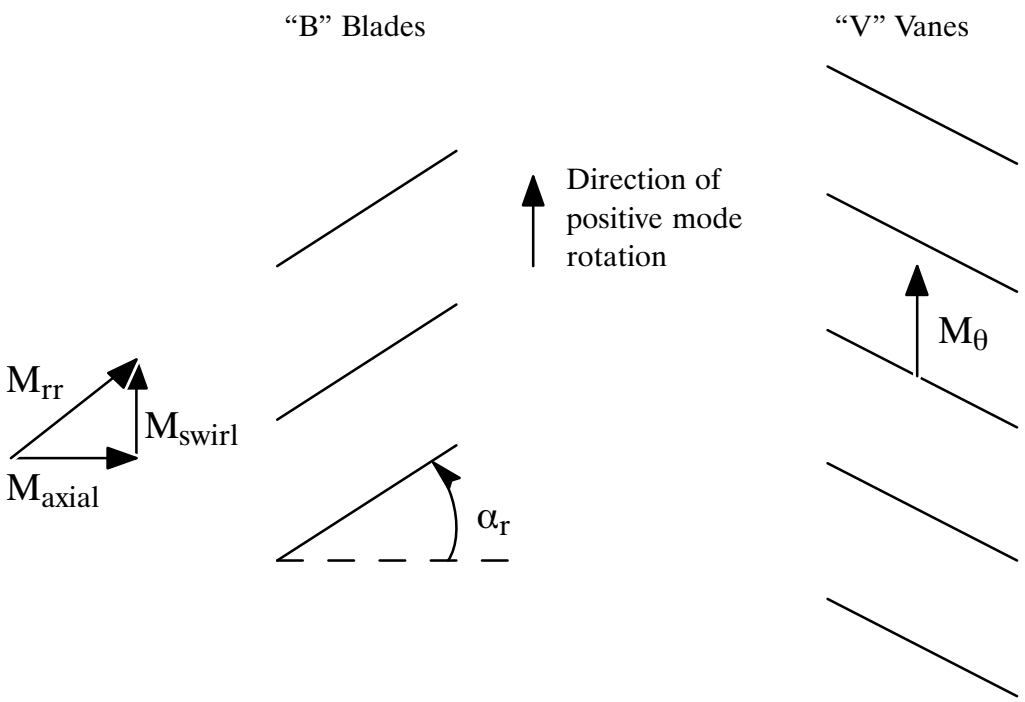

Figure 2 Geometry for the rotor

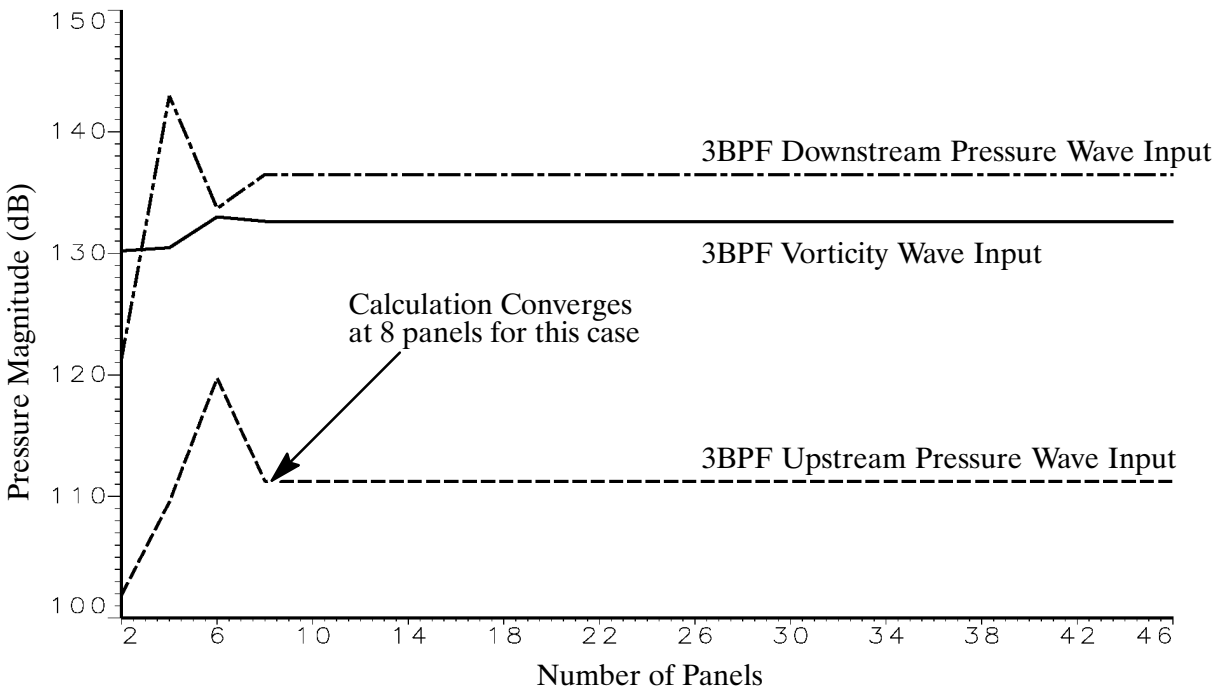

Figure 3 Sample far field pressure magnitude for the stator: upstream pressure output

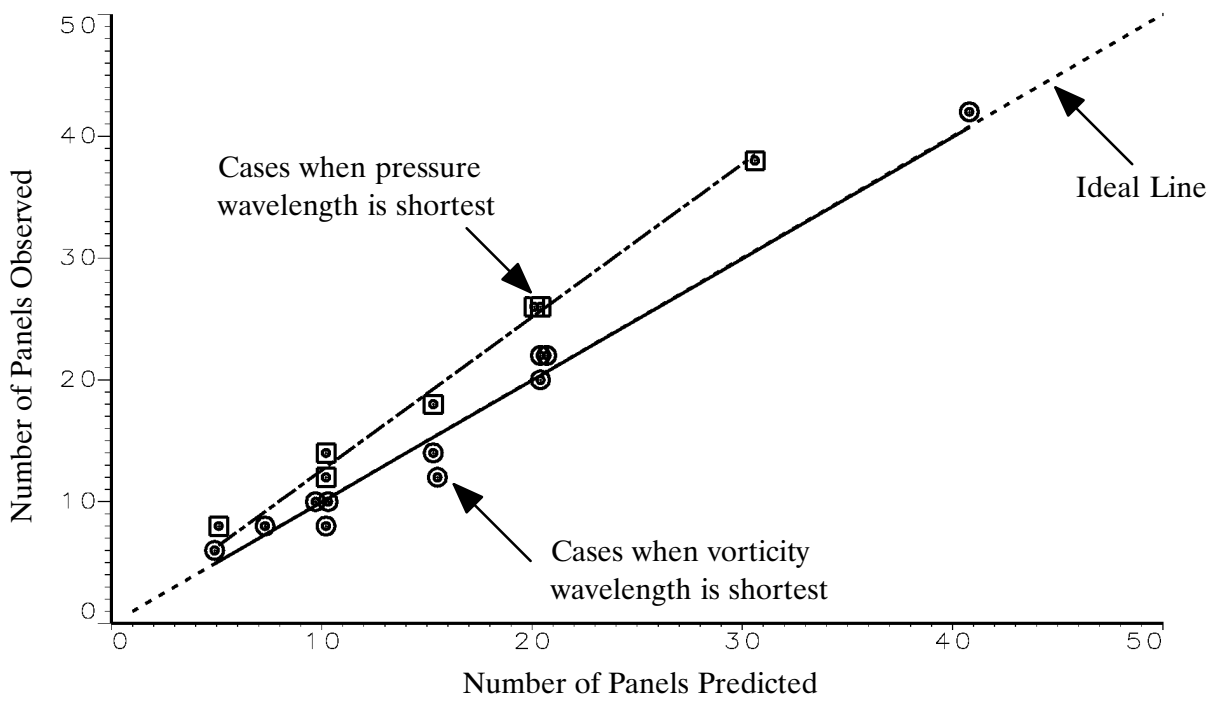

Figure 4 Vorticity Criterion Results on the Stator

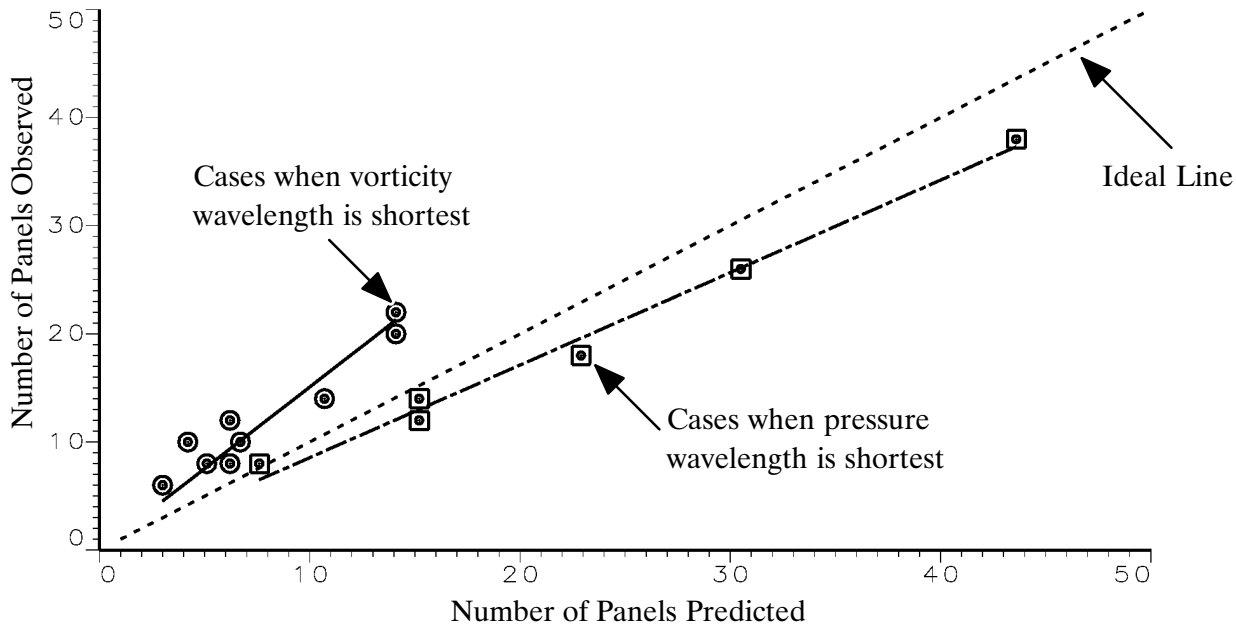

(a) Last Cuton Mode Criterion

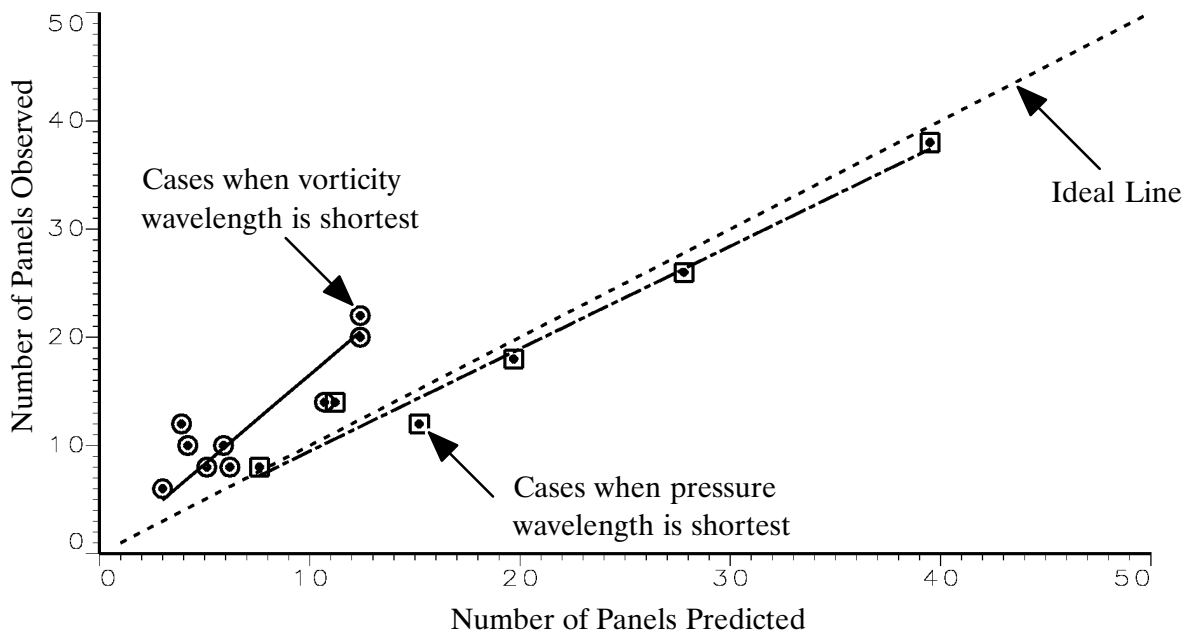

(b) Maximum K_{mn} Criterion

Figure 5 Pressure Wave Criteria Results on the Stator

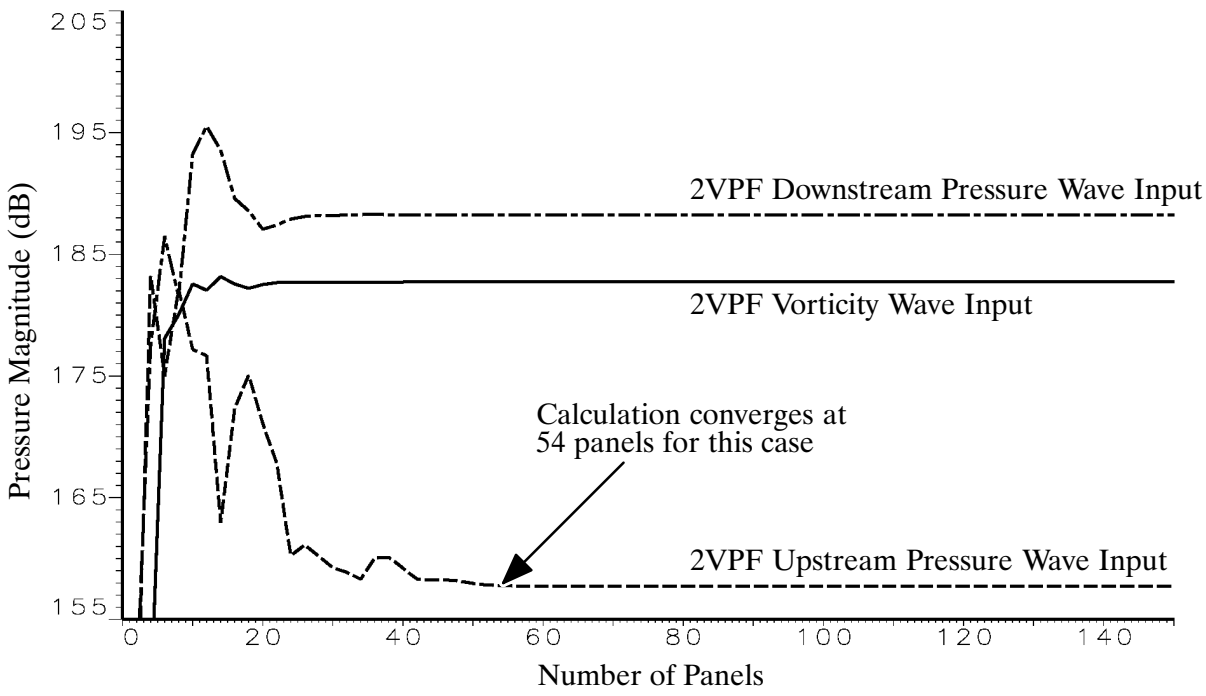

Figure 6 Sample far field pressure magnitude for the rotor: upstream pressure output

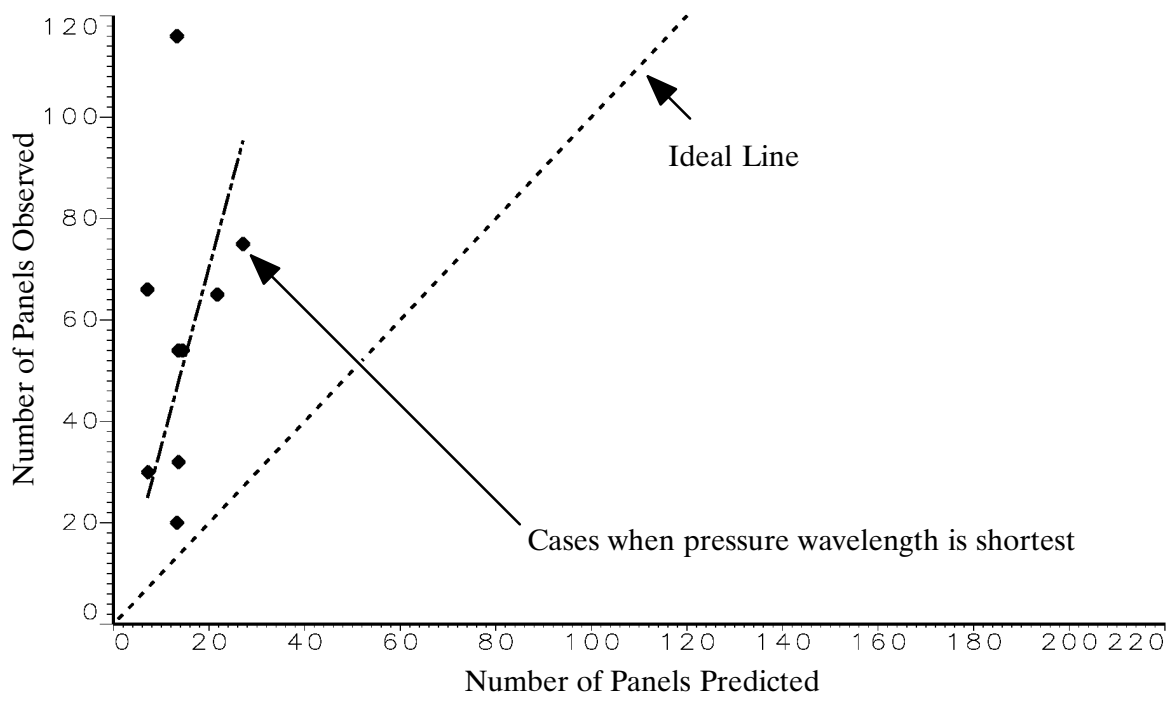

Figure 7 Vorticity Criteria results on the rotor

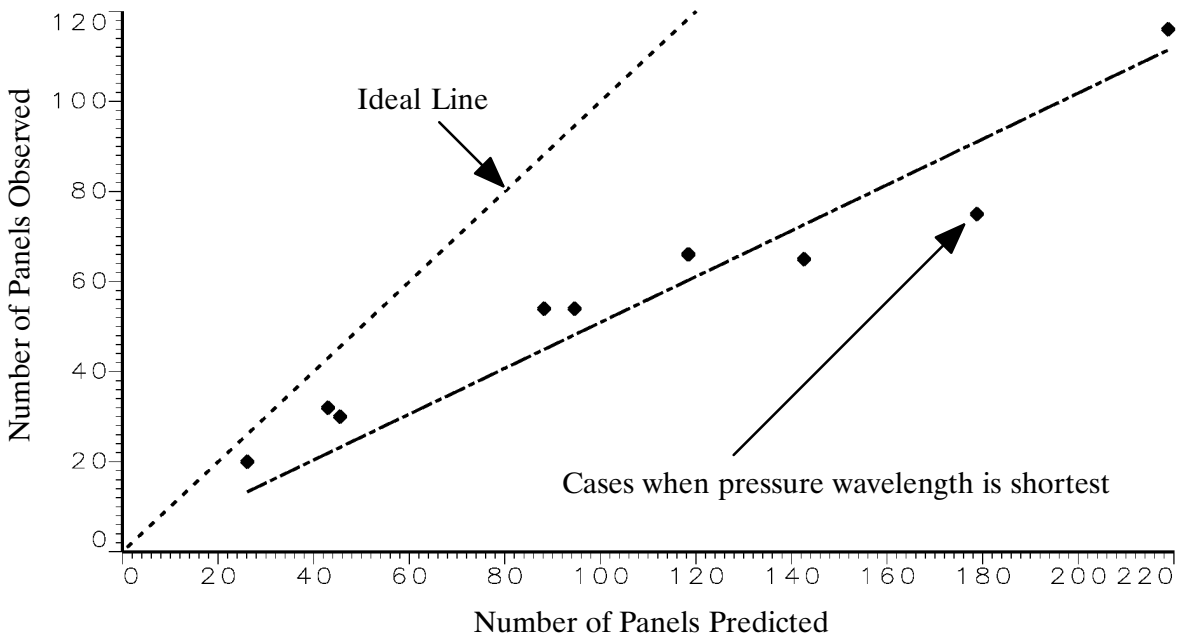

(a) Predicted Pressure Wave Criterion − Last Cuton Mode

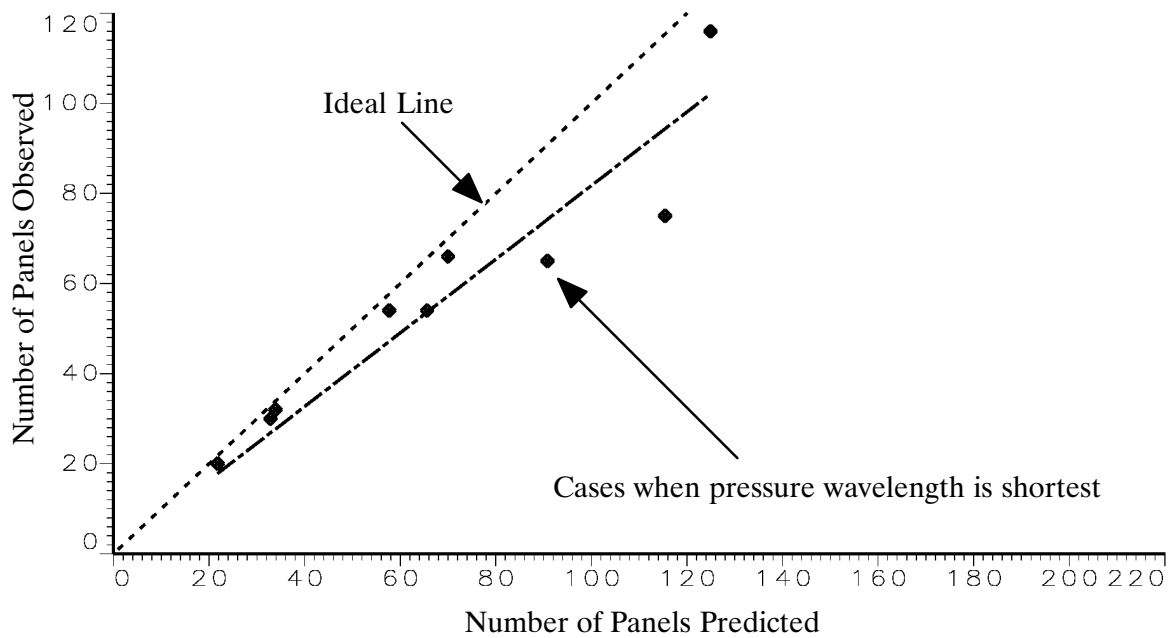

(b) Predicted Pressure Wave Criterion − Max K_{mn}

Figure 8 Pressure wave criteria results on the rotor

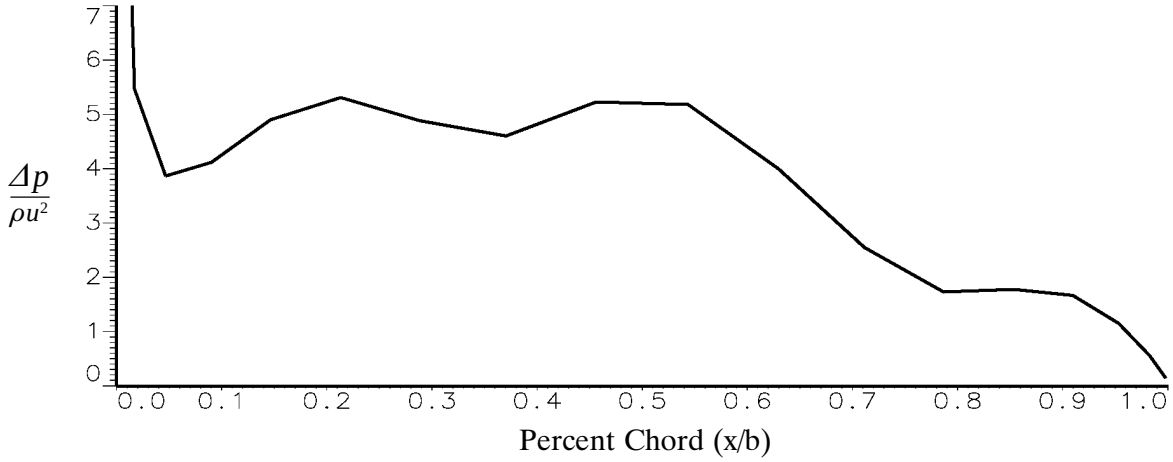

(a) Unsteady Pressure Distribution with 18 Panels (selected by the criterion)

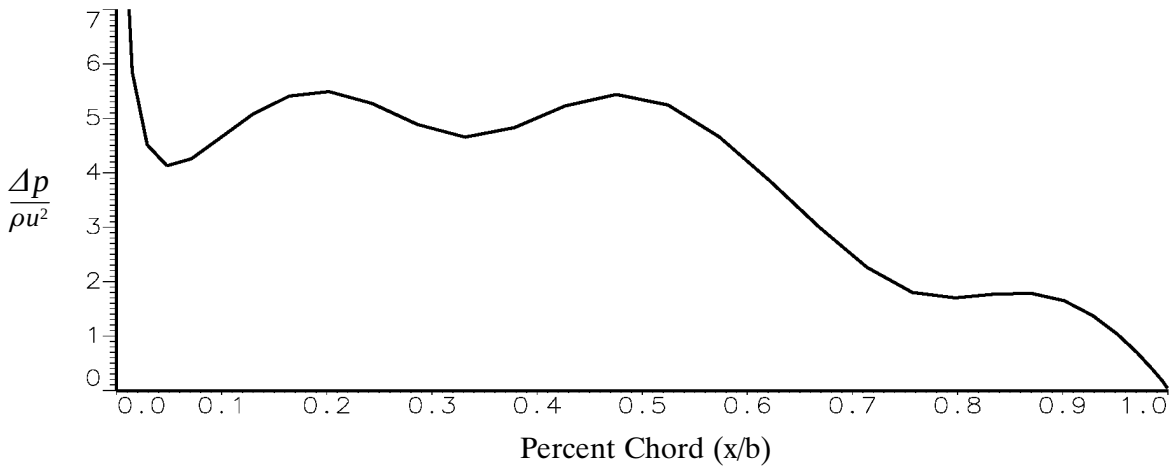

(b) Unsteady Pressure Distribution with 32 Panels

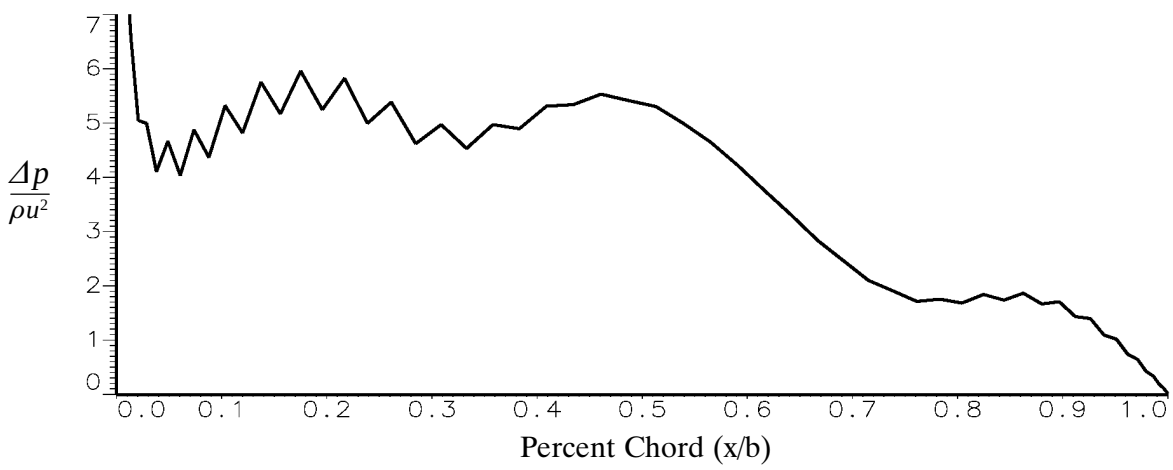

(c) Unsteady Pressure Distribution with 60 Panels showing signs of an instability

Figure 9 Unsteady pressure distribution on the rotor tip at BPF; N_{1C} = 9600 rpm

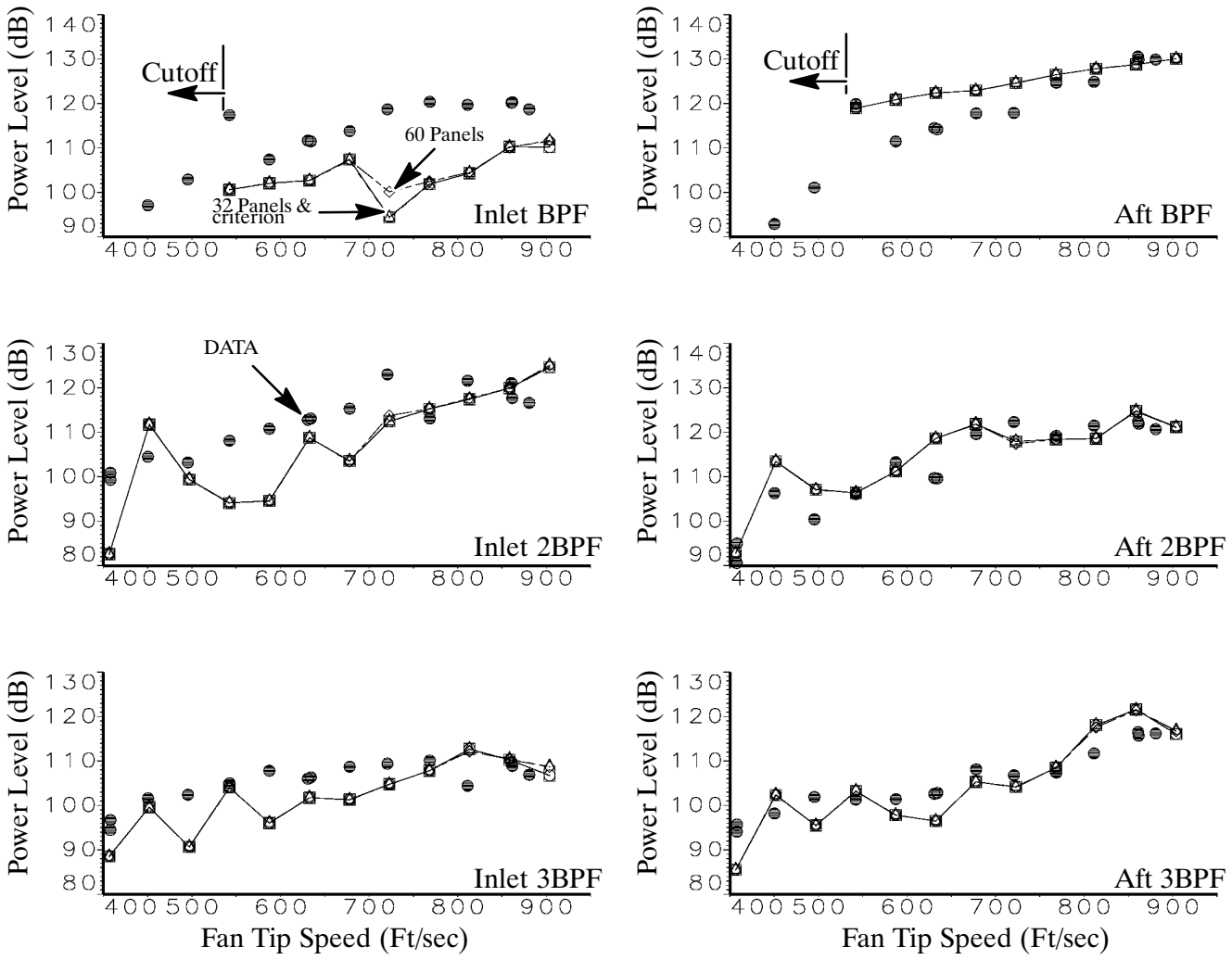

Figure 10 TFaNS power level predictions: comparison of different SOURCE3D runs

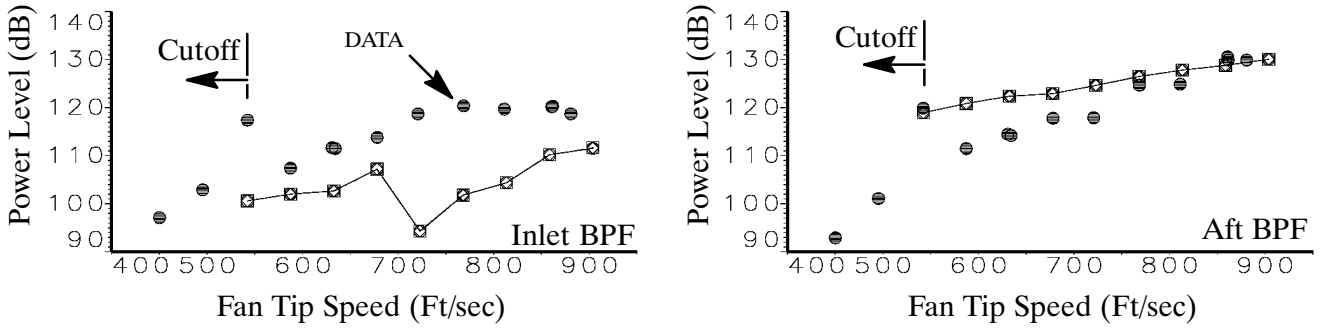

Figure 11 TFaNS power level predictions: comparison of maximum number of panels allowed

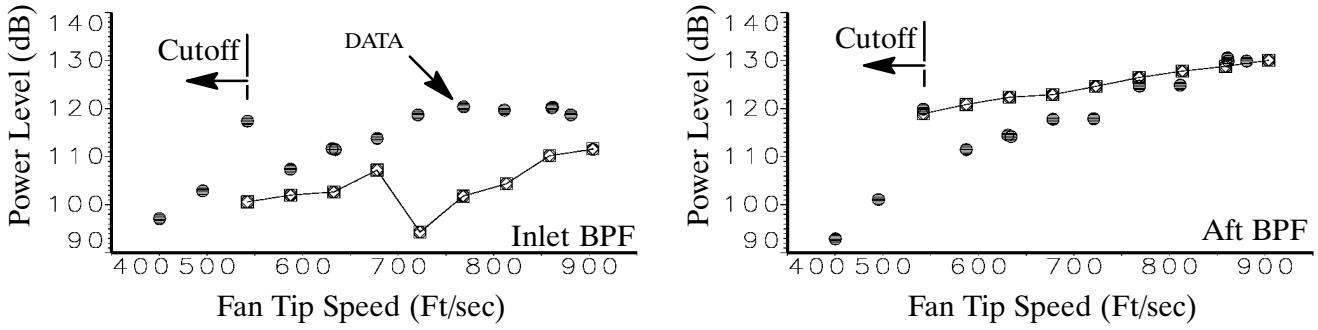

Figure 12 TFaNS power level predictions: comparison of different convergence terms

REPORT DOCUMENTATION PAGE

Form Approved
OMB No. 0704-0188

Public reporting burden for this collection of information is estimated to average 1 hour per response, including the time for reviewing instructions, searching existing data sources, gathering and maintaining the data needed, and completing and reviewing the collection of information. Send comments regarding this burden estimate or any other aspect of this collection of information, including suggestions for reducing this burden, to Washington Headquarters Services, Directorate for Information Operations and Reports, 1215 Jefferson Davis Highway, Suite 1204, Arlington, VA 22202-4302, and to the Office of Management and Budget, Paperwork Reduction Project (0704-0188), Washington, DC 20503.

1. AGENCY USE ONLY (*Leave blank*)

2. REPORT DATE
March 1999

3. REPORT TYPE AND DATES COVERED
Final Contractor Report

4. TITLE AND SUBTITLE
TFaNS Tone Fan Noise Design / Prediction System
Volume III: Evaluation of System Codes

5. FUNDING NUMBERS
WU–538–03–11–00
NAS3–26618

6. AUTHOR(S)
David A. Topol

7. PERFORMING ORGANIZATION NAME(S) AND ADDRESS(ES)
United Technologies Corporation
Pratt & Whitney
400 Main Street
East Hartford, Connecticut 06108

8. PERFORMING ORGANIZATION REPORT NUMBER
E–11618

9. SPONSORING/MONITORING AGENCY NAME(S) AND ADDRESS(ES)
National Aeronautics and Space Administration
John H. Glenn Research Center at Lewis Field
Cleveland, Ohio 44135–3191

10. SPONSORING/MONITORING AGENCY REPORT NUMBER
NASA CR—1999-208884
PWA 6420–103

11. SUPPLEMENTARY NOTES
Project Manager, Dennis L. Huff, NASA Lewis Research Center, organization code 5940, (216) 433–3913.

12a. DISTRIBUTION/AVAILABILITY STATEMENT
Unclassified - Unlimited
Subject Category: 71 Distribution: Nonstandard

This publication is available from the NASA Center for AeroSpace Information, (301) 621–0390.

12b. DISTRIBUTION CODE

13. ABSTRACT ***(Maximum 200 words)***

TFaNS is the Tone Fan Noise Design/Prediction System developed by Pratt & Whitney under contract to NASA Lewis (presently NASA Glenn). The purpose of this system is to predict tone noise emanating from a fan stage including the effects of reflection and transmission by the rotor and stator and by the duct inlet and nozzle. These effects have been added to an existing annular duct/isolated stator noise prediction capability. TFaNS consists of: The codes that compute the acoustic properties (reflection and transmission coefficients) of the various elements and write them to files. CUP3D: Fan Noise Coupling Code that reads these files, solves the coupling problem, and outputs the desired noise predictions. AWAKEN: CFD/Measured Wake Postprocessor which reformats CFD wake predictions and/or measured wake data so it can be used by the system. This volume of the report evaluates TFaNS versus full-scale and ADP 22" rig data using the semi-empirical wake modelling in the system. This report is divided into three volumes: Volume I: System Description, CUP3D Technical Documentation, and Manual for Code Developers; Volume II: User's Manual, TFaNS Vers. 1.4; Volume III: Evaluation of System Codes.

14. SUBJECT TERMS
Acoustics; Turbomachinery; Noise; Fans

15. NUMBER OF PAGES
59

16. PRICE CODE
A04

17. SECURITY CLASSIFICATION OF REPORT
Unclassified

18. SECURITY CLASSIFICATION OF THIS PAGE
Unclassified

19. SECURITY CLASSIFICATION OF ABSTRACT
Unclassified

20. LIMITATION OF ABSTRACT